

Formation of Ozone and PM_{2.5} in Smoke from Prescribed Burning in the Southeastern United States

Published as part of ACS ES&T Air *special issue* "Wildland Fires: Emissions, Chemistry, Contamination, Climate, and Human Health".

Rime El Asmar, Zongrun Li, Haofei Yu, Susan O'Neill, David J. Tanner, L. Gregory Huey, M. Talat Odman, and Rodney J. Weber*



Cite This: <https://doi.org/10.1021/acsestair.4c00231>



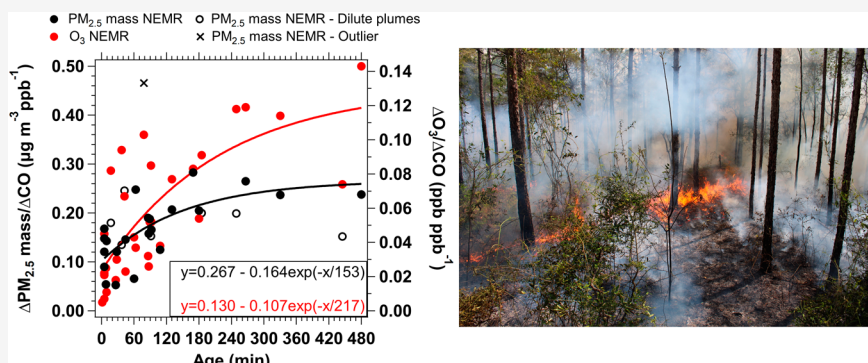
Read Online

ACCESS |

Metrics & More

Article Recommendations

Supporting Information



ABSTRACT: Ground-based measurements of smoke from prescribed fires in the southeastern US during the burning seasons of 2021 through 2024 are used to assess ozone (O₃) and PM_{2.5} mass formation and their changes with age in 69 smoke events. O₃ production occurred in nearly all plumes (31 out of 32) measured between 12:00 and 18:00. The O₃ to carbon monoxide ratio ($\Delta\text{O}_3/\Delta\text{CO}$) increased from 5.32 to 143 ppb ppm⁻¹ as plumes aged from 1 to 480 min, showing a rapid initial increase, doubling in approximately 60 min, followed by a gradual slow down. Residual O₃ from daytime fires was detected during the evening and night, disrupting the typical nighttime O₃ pattern. The $\Delta\text{PM}_{2.5}\text{ mass}/\Delta\text{CO}$ ratio ranged from 40.6 to 466 $\mu\text{g m}^{-3}$ ppm⁻¹. Little age-related change was observed in smoke measured at night with $\Delta\text{PM}_{2.5}\text{ mass}/\Delta\text{CO}$ levels similar to those observed at the time of emissions (132 $\mu\text{g m}^{-3}$ ppm⁻¹). However, in plumes of observed O₃ enhancement during photochemically active periods (12:00–18:00), $\Delta\text{PM}_{2.5}\text{ mass}/\Delta\text{CO}$ followed a similar increasing trend as $\Delta\text{O}_3/\Delta\text{CO}$, and the two were correlated ($r^2 = 0.5$), although the O₃ trend was more pronounced. For these data, a stronger correlation between $\Delta\text{PM}_{2.5}\text{ mass}/\Delta\text{CO}$ and age was found in plumes of higher PM_{2.5} concentration (PM_{2.5} mass > 35 $\mu\text{g m}^{-3}$). The impact of the prescribed burning season in the southeast was evident in state-operated air quality monitors near burning areas, where PM_{2.5} mass concentrations were 25–30% higher than nonburning seasons. In contrast, changes in daily maximum 8 h O₃ concentrations were less pronounced. Our data indicates that the formation of both O₃ and PM_{2.5} frequently occurred in smoke from prescribed fires during photochemically active periods in the studied regions. These findings are significant, as exposure to O₃ and PM_{2.5} can negatively impact human health.

KEYWORDS: smoke, prescribed fires, emissions, evolution, PM_{2.5} mass, ozone, southeast USA

1. INTRODUCTION

Biomass burning is a major source of atmospheric trace gases and particles that can impact air quality^{1,2} through direct emissions of gases and particles and the conversion of emissions to secondary species, including ozone (O₃) and aerosols.^{3–6} Emissions from wildfires significantly impact local and regional air quality in the United States (US) due to their growing frequency and intensity in recent decades.^{7–9} While natural fires can be beneficial for the ecosystems,¹⁰ contemporary wildfires pose a major threat to the environment,

causing destruction of infrastructure, loss of habitats, soil erosion, and widespread degradation in water and air quality. For these reasons, prescribed burning, which is the intentional

Received: September 2, 2024

Revised: January 17, 2025

Accepted: January 21, 2025

ignition of controlled fires, is being used for restoration of ecosystems, land management, and reduction of fuels to lower the impacts of wildfires and so is anticipated to increase.^{11,12} According to the National Interagency Fire Center, prescribed burning was conducted on 23 million ha during the period 1998 to 2018 in the US, with an approximately 5% annual increase.¹¹ Southeastern US accounted for 70% of area burnt and 98% of the observed annual increase over the last 20 years,¹¹ and earlier decades,¹³ which may account for fewer severe wildfires occurrences in the region.^{14–16} Prescribed burning is applied when there are favorable conditions, which depends on the types of fuel, and moisture content, weather, and dispersion conditions. However, it can still significantly impact air quality, and the favorable conditions of clear weather for burning may also lead to formation of secondary species, such as O₃ and PM_{2.5}. Given the ongoing rise in the use of prescribed burning and its potential impact on air quality, many studies have been conducted to measure and estimate the emissions from different prescribed fires in the US.^{4,17–19}

O₃ is a secondary pollutant, formed in the troposphere through photochemical reactions involving the oxidation of volatile organic compounds (VOCs) in the presence of nitrogen oxides (NO_x) and sunlight.^{20,21} Biomass burning emits large amounts of NO_x, VOCs, and species such as formaldehyde (HCHO) and nitrous acid (HONO) that under photochemically active conditions can rapidly produce radicals that initiate O₃ production.²² O₃ can form as plumes age and smoke is transported over distances from the burning area^{23,24} and can impact urban O₃ concentrations when smoke rich in VOCs mix with other urban emissions, particularly NO_x.^{23,25,26} In addition to O₃, fires produce particulate matter (PM), mostly PM_{2.5} (PM with an aerodynamic diameter of 2.5 μm or smaller). PM_{2.5} from wildland fires has also been found to have air quality impacts over large spatial scales.^{23,27,28} A major component of biomass burning PM_{2.5} is the carbonaceous matter which is composed of organic carbon (OC) and elemental carbon (EC).²⁹ Organic carbon, including light absorbing species called brown carbon (BrC), originates from both primary and secondary photochemical reactions,^{30,31} while EC, or black carbon (BC), also produced from incomplete combustion, is primary.³² Primary and secondary inorganic PM_{2.5} species are also emitted and produced from biomass burning emissions, such as metals (e.g., iron, potassium)^{33,34} and ammonium nitrate.³⁵

Wildland fire smoke spreads over the near-fire, regional and large spatial scales leading to the potential of exposure to smoke and its products by a large population. O₃ can cause serious adverse health impacts. Due to its high reactivity, inhaled O₃ causes irritation in the respiratory system triggering inflammation, increasing the risk of respiratory infections like bronchitis and pneumonia, and permanent damage to the lungs and chronic respiratory problems like asthma.^{36–39} PM_{2.5} on its own is viewed as more dangerous than O₃ exposures,⁴⁰ and is linked to a wide range of adverse outcomes, such as adverse respiratory effects, cardiovascular and neurological diseases, and an increased risk of adverse birth outcomes.^{41–44} Exposure to both O₃ and PM_{2.5} have been shown to have a combined synergistic adverse health effects,^{45,46} and measurements show aged biomass burning PM_{2.5} on its own may be more detrimental due to higher aerosol oxidative potential and reactive oxygen species concentrations.^{47–50}

Here, we show results from a 4-year study of air quality in prescribed burning areas in the southeastern USA. A series of measurements in the prescribed fire seasons were taken during 5 campaigns between 2021 and 2024, providing a data set on many recorded smoke events. The aim of this study is to characterize the evolution of O₃ and PM_{2.5} from prescribed fires in a specific region of the southeastern USA.

2. METHOD

2.1. Site Description. Prescribed fires at three US Army Bases in the southeastern US were studied during the late winter to early spring (February to May) burning seasons of 2021 through 2024. Most data from the 2021 and 2022 period involved 5 sampling trailers deployed at different sites throughout Fort Moore Army Base (formerly Fort Benning) in west central Georgia, US (Figures S1 and S2). The site deployment dates and sampling locations are described elsewhere.⁵¹ We utilized a passive monitoring approach at Fort Moore, involving continuous measurements throughout most of the approximately 4-month burning period (January to May). Prescribed burning has been used as a land management tool at the 74000 ha military base, with 59000 ha of forested lands dominated by longleaf pine. This practice has been used to reduce wildfire frequency and has also served ecological purposes, such as maintaining habitat for red-cockaded woodpeckers. Approximately 12000 ha are currently burned annually, with plans to increase to ~18000 ha in the future. Not all smoke events detected at Fort Moore were due to fires on the base; burning occurs in the region around the Fort during periods when burning is also occurring at the Fort.⁵¹ In addition to the long period of sampling at Fort Moore, two intensive short (2 to 3 days) multi-investigator field studies were conducted at Fort Stewart Army Post in southeast Georgia, US, in March 2022 and February 2024. The Fort Stewart daily average prescribed burn area is 240 ha, with a goal to reach 40000 to 49000 ha every year throughout the 110000 ha base. Approximately 97000 ha of the base consists of upland and flatwood pine forest, forested wetlands, and open areas. A similar intensive field study took place at Eglin Air Force Base (AFB), located in the western Florida Panhandle, from March 10 to 20, 2023. Of the 190000 ha, approximately 120000 ha is forested with longleaf pine, and approximately 36000 ha are burned annually. For the intensive short studies at Fort Stewart and Eglin AFB, the measuring approach was based on positioning one or two instrumented trailers at locations predicted to intercept smoke plumes in the day prior to the planned burn, in contrast to the passive approach of the Fort Moore study.

2.2. Instrumentation. To characterize the prescribed fire smoke, the trailers were equipped with several instruments sampling through inlets ~4.0 m above ground level and 1.5 m above the trailer roof. Measurements included carbon monoxide (CO), nitrogen oxides (NO, NO_x), ozone (O₃), PM_{2.5} mass concentration, and particle light absorption coefficients at multiple wavelengths.

CO was measured using IR analyzers (Thermo Fisher Scientific Inc., model 48C, Franklin, MA) with custom-built CO scrubbers made of 0.50% Pd on alumina catalyst heated to 180 °C.⁵¹ O₃ was measured using ultraviolet (UV) photometric analyzers (Thermo Fisher Scientific Inc., model 49C, Franklin, MA) zeroed through an internal O₃ scrubber, and NO_x species were measured using chemiluminescence NO–NO₂–NO_x analyzers (Thermo Fisher Scientific Inc., model

42i, Franklin, MA), which have an LOD of 0.40 ppb. NO_x analyzers were calibrated automatically every 6 h, using NO and NO₂ calibration standards purchased from Airgas (Radnor, PA).

PM_{2.5} mass concentration was determined using a Tapered Element Oscillating Microbalance (TEOM) series 1400a ambient particulate monitor (Thermo Fisher Scientific, Franklin, MA) with inlet temperature of 50 °C. A PM_{2.5}-cut cyclone (URG 2000 = 30EH 16.7 LPM 2.5 μm) was located upstream of the optical measurements. Black carbon (BC) mass concentration was determined in the various trailers as follows; two trailers had 7-wavelength aethalometers, one had 2-wavelength aethalometer, and the other two had single-wavelength particle soot absorption photometers (PSAPs).

Light absorption by PM_{2.5} organic species, BrC, here defined as the light absorption at 365 nm was calculated from the 7-wavelength aethalometer data⁵¹ and was used as a smoke tracer. Only multiwavelength aethalometers (AE33 and AE31) were utilized at Fort Stewart and Eglin AFB. More details, including LODs, calibrations, and data corrections are described in El Asmar et al.⁵¹

2.3. Tools and Analysis Methods. Smoke Events Identification. The analysis is based on combining the results of various smoke plumes detected at Fort Moore during two years of passive sampling, plus the plumes from the three intensive studies (two at Fort Stewart and one at Eglin AFB). In the passive sampling approach used at Fort Moore, we focus on smoke that could be clearly identified as coming from active burning, since background concentrations of PM_{2.5} can fluctuate due to the influence of smoke from burns on previous days. Smoke events were identified by an increase in 20 min averaged PM_{2.5} mass concentration above 25 μg m⁻³ which was always accompanied by an increase in CO and BC concentrations and BrC absorption. This categorization also excludes short transient events from local sources, such as a passing vehicle that can be encountered at measuring sites near training areas on military bases. All days without smoke events (i.e., days without 20 min averaged PM_{2.5} mass concentration above 25 μg m⁻³) were used to assess typical regional ambient concentrations; however, it is acknowledged that these periods may still include times with lesser impacts from fire emissions.

The duration of each smoke event was estimated from the time when PM_{2.5} mass and CO concentrations began rising above the concentration before the event until they returned to typical levels and remained stable. For the studies at Fort Stewart and Eglin AFB in 2022 through 2024, sampling trailers were positioned to measure smoke from prescribed fires that were set at a known place and time. Overall, 69 smoke events were recorded, of which some can be sourced to the same fires but were monitored multiple times at the same or at different trailers. Table S1 summarizes the smoke events with their corresponding dates, times, locations, estimated smoke age, and maximum PM_{2.5} mass concentrations.

Since the focus of this work is on studying the production of secondary species, of the 69 smoke events we selected those that had a clear O₃ enhancement, using this as an indicator of postemission chemistry (31 of the 69 showed evidence of enhanced O₃). O₃ enhancement was identified by an increase in O₃ concentration above the undisturbed level just prior or after the enhancement, along with simultaneous increase in measured smoke related species (CO, BC, and BrC) confirming it was a smoke event. All smoke events with O₃ enhancement had PM_{2.5} mass concentration above 25 μg m⁻³.

Normalized Excess Mixing Ratio (NEMR). NEMR was used to account for dilution of species in smoke plumes. It is the ratio of the enhancement of species of interest, Y, to the enhancement of a coemitted reference species, X. For example, the NEMR of species Y is expressed as the ratio ΔY/ΔX. Here ΔY and ΔX represent the concentrations of Y and X after subtracting the background concentrations (those expected if the smoke was not present). CO is used as the reference species (X) to track the movement and dispersion of smoke,^{3,52} since it is relatively long-lived (~1 month lifespan), and coemitted during incomplete combustion. For PM_{2.5} and CO, the increase relative to background is clear and so we used the average of the measurements before and after the smoke event as the background and subtract this constant value from the data in the plume. For O₃, determining the background can be more difficult since it can vary significantly relative to the enhancement that may occur in the smoke plume. When the smoke plume began and ended during the day and when O₃ background levels are generally high and not dramatically changing (12:00–18:00), the background concentration was calculated at each measurement point using a linear relationship between the first and last point prior to and after detection of the peak as illustrated for the first shaded region of Figure S3. We restrict our analysis to the period between 12:00 and 18:00 since this is the photochemically active period (Figure S4), without the rapid changes in background O₃ (e.g., in the morning between 10:00 and 11:00, Figure S4), which would introduce uncertainty in calculating the O₃ enhancement from smoke. In cases where only the beginning or end of the smoke events coincide with the high O₃ episode, the background is not as obvious. In these cases, where the background O₃ is changing rapidly near the time the smoke plume is first detected or dissipating (identified by CO, PM_{2.5} mass, BC, and BrC), the O₃ concentration when the transition is not occurring is used as the background value, and this value is subtracted from O₃ measured during the event, as illustrated in the second shaded region of Figure S3. In 31 of 32 studied smoke events (restricted to times between 12:00 and 18:00), O₃ was always higher than the background levels (ΔO₃ for all studied smoke events is positive), however, O₃ background levels are relatively high compared to O₃ produced in plumes, unlike other species with lower background levels relative to concentrations in smoke plumes, making them more uncertain than ΔCO, ΔPM_{2.5} mass, ΔBC, and ΔBrC. When smoke events began before or extended beyond the high O₃ phase in the diurnal cycle (i.e., 12:00 to 18:00), only the data during this high phase period was used for NEMR determination and for studying variation with age.

Smoke Source and Age Determination. Smoke sources and plume ages were determined using the average measured wind vector and distance from the smoke source to the measurement. Of the 69 smoke events studied, 8 were unidentified due to mismatches between the detected fires and wind direction, and 10 additional events had no age prediction due to unavailable wind data. A detailed description of the method can be found in El Asmar et al.⁵¹

3. RESULTS

3.1. Correlation among Emitted Species in Smoke Events. During the study, smoke plumes were readily identified by a simultaneous increase in concentrations of CO, and PM_{2.5} mass and BC concentration, and PM_{2.5} BrC (light absorption coefficient at 365 nm wavelength). Some

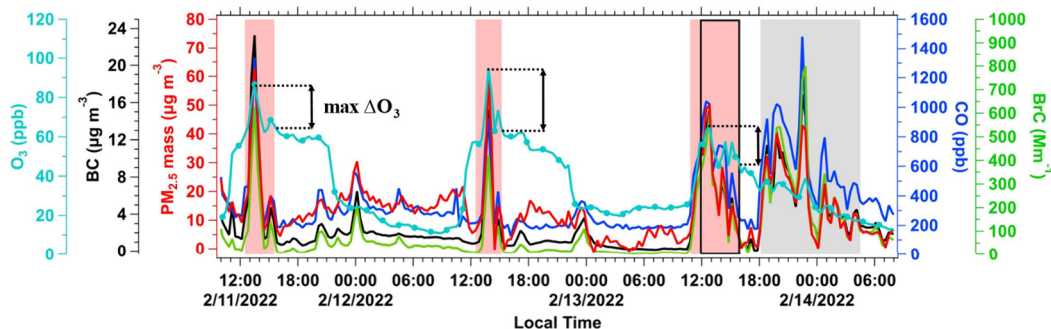


Figure 1. A time series showing maximum O_3 enhancements (black double-headed arrows) when smoke was detected on February 11, 12, and 13, 2022, at Fort Moore. Red shaded areas correspond to the 3 daytime smoke events, while the gray shaded area corresponds to the nighttime smoke event discussed. The black box highlights the portion of the event used for studying O_3 enhancement (i.e., beginning after 12:00), see Figure S3 for more details. Measurement time resolution is 20 min for CO, O_3 , PM_{2.5} mass, BC, and BrC.

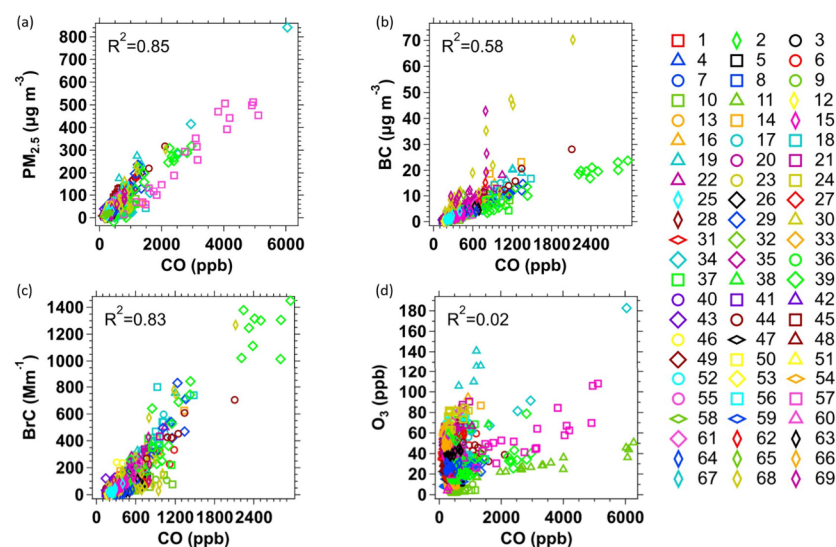


Figure 2. Correlations between (a) PM_{2.5} mass, (b) BC, (c) BrC, and (d) O_3 and CO for all data of smoke events studied and summarized in Table S1. Different colors and shapes correspond to different smoke plumes. All data are averages over a 20 min period.

smoke events also had O_3 peaks superimposed on a broader regional daytime O_3 concentrations. For example, Figure 1 shows a representative example of a time series of smoke events measured at one site during 3 days at Fort Moore. At Fort Moore, prescribed burning is generally initiated between morning and noon, with smoke events detectable throughout the day. The smoke events in Figure 1 were recorded in the afternoon to evening period. Smoke events can also be observed at other times due to smoldering fires that continue into the night or the next day. Because of this, and along with residual smoke from prior fires, numerous enhancements in smoke species were also observed at night. For example, this is observed following the third peak in Figure 1 between 18:00 on February 13, 2022, and 4:30 the next morning on February 14, 2022. This night-time smoke is believed to be from fires from the previous day.

The contrasts in O_3 and PM_{2.5} mass concentrations between periods with and without smoke are notable. Figure 1 shows that O_3 often has a clear diurnal trend, characteristic of regional O_3 production, and superimposed on this is an O_3 enhancement when smoke is detected. PM_{2.5} mass can vary substantially during the nonsmoke periods (defined here as PM_{2.5} mass below 25 $\mu\text{g m}^{-3}$). Small peaks from smoke are seen in Figure 1 (spikes in CO, BC, BrC, and PM_{2.5} mass) and

contrast with the substantial increases in PM_{2.5} mass observed during a smoke event. Without smoke, a typical clear-day diurnal profile of O_3 is shown in Figure S4.

The time series of smoke events in Figure 1 also show high correlations between the various measured parameters in the smoke plumes. Combining measurements from all smoke events recorded in this study, Figure 2 shows that there are high correlations between CO and PM_{2.5} mass, BC, and BrC, and poorer correlation between CO and O_3 . The much higher O_3 variability relative to CO between individual smoke events may be expected due to the inclusion of nondaylight smoke events and the fact that O_3 , as a secondary species, often shows plume enhancements (when CO is also elevated) against a large regional O_3 background during daytime smoke events. The slopes of the various species shown in Figure 2 represent the species NEMRs relative to CO. Some species, such as BC, show a few outlier data points with BC NEMRs reaching 0.043 and 0.035 $\mu\text{g m}^{-3} \text{ ppb}^{-1}$. The NEMRs recorded in this study for PM_{2.5} mass, BC, and BrC are similar to those reported in other studies, as shown in the detailed comparison by El Asmar et al.⁵¹

3.2. O_3 and PM_{2.5} Mass Background Concentrations. Concentrations of O_3 and PM_{2.5} mass are perturbed by the smoke events relative to typical conditions. We provide data on

Table 1. Monthly Median Concentrations of O₃ (ppb) and PM_{2.5} Mass (μg m⁻³) at T Main, T 1293, and T 1291 During the 2022 Campaign at Fort Moore, Excluding Days when Significant Smoke was Detected, i.e., Days Are Excluded When the Maximum 20 Min Averaged PM_{2.5} Mass Was Greater than 25 μg m⁻³^a

month/year	trailer	daytime O ₃ ppb	nighttime O ₃ ppb	daytime PM _{2.5} mass concentration μg m ⁻³	nighttime PM _{2.5} mass concentration μg m ⁻³
February 2022	T Main	45.91	24.55	0.58	2.75
March 2022	T Main	46.44	15.94	0.90	2.77
	T 1293	40.03	21.29	4.16	5.22
	T 1291	45.24	32.56	4.32	7.88
April 2022	T Main	53.59	29.87	1.80	2.05
	T 1293	44.17	23.25	5.36	5.36
May 2022	T Main	43.73	25.46	0.76	2.79
	T 1293	37.98	20.19	6.89	6.71
	T 1291	36.45	22.02	4.18	7.73

^aDaytime and nighttime median concentrations were calculated from measurements between 13:00–18:00 and 00:00–05:00, respectively. The locations of trailers are shown in Figure S2.

background conditions here as a reference for comparison to the smoke events by looking at conditions at Fort Moore when no large fires were detected (i.e., days when 20 min average PM_{2.5} mass concentration never exceeded 25 μg m⁻³). Typically, in this region when smoke impacts are not large, surface O₃ concentration starts increasing at ~8:30 to 10:30 local time reaching the high O₃ period of the diurnal cycle at ~11:30 to 12:30 (some of the variability is due to changes with time of year). Concentrations then decrease rapidly at ~19:00 to 21:00 and remain low for the rest of the night. For a broader contrast between day and night, at Fort Moore during nonsmoke periods, the median O₃ concentrations for non-smoke periods are 46.4 ppb (interquartile range (IQR) = 14.6 ppb) during the day (13:00 to 18:00) and 23.3 ppb (IQR = 12.6 ppb) during the night (00:00 to 05:00). The diurnal trend evident on clear days is due to its photochemical production, leading to a good correlation with solar radiation ($r^2 = 0.66$, Figure S5). Table 1 shows a longer time-scale trend throughout the burning season. Average daytime O₃ concentration for those nonsmoke event periods increased from February to April, followed by a decrease in May (median daytime O₃ concentration for February, March, April, and May was respectively 45.9, 46.4, 53.6, and 43.7 ppb at trailer T Main, see Figure S2). This could be attributed to the increase in the area burned regionally during these months, which affects the overall background O₃ concentrations, combined with the increase in solar radiation transitioning from February to May. For instance, at Fort Moore in 2022, the area burned was 1,800 ha in February, 5,600 ha in March, 1,800 ha in April, and 430 ha in May. The daily average solar radiation was 3.2, 4.3, 4.9, and 6.6 kW hr m⁻² for February, March, April, and May, respectively.

The monthly medians of PM_{2.5} mass concentrations during nonsmoke event periods are also shown in Table 1 and range from approximately 0.60 to 6.9 μg m⁻³ during the day (monthly means range from 0.80 to 7.0 μg m⁻³) and from approximately 2.1 to 7.9 μg m⁻³ at night (monthly means range from 2.3 to 7.9 μg m⁻³) across three sites at Fort Moore in 2022. (Note, the lower ranges are below our measured 20 min averaging time LOD of 5.6 μg m⁻³, but higher than the manufacturers stated LOD. Since this is highly averaged data, we report concentrations below our measured LOD). Higher concentrations at night may be due to residual smoke from burning throughout the region, a shallow boundary layer, as well as decreased aerosol evaporation due to lower temperatures. Additionally, there was a moderate spatial variability

among the sites within and outside Fort Moore. Higher background levels were measured at sites near the main road and training areas (T 1291 and T 1293) compared to T Main (see Figures S1 and S2 for map with site locations), which was located further from these areas. The monthly mean concentration on days without smoke events recorded at two state monitoring sites at Columbus airport and Phenix City South Girard School (see Figure S2a for locations) ranged between 7 and 9 μg m⁻³. Higher background PM_{2.5} mass concentrations at these sites relative to those within the Fort are likely attributed to the local urban sources in contrast to the more remote sampling locations at the Fort. The O₃ and PM_{2.5} mass concentration data from these state sites are used for a regional assessment of prescribed burning in section 4.

3.3. Ozone and PM_{2.5} Mass Enhancement in Plumes from Prescribed Fires. *Ozone Enhancement.* Postemission chemistry can significantly affect the impact of smoke from fires on exposed populations.^{47,49} In this study, as noted above, measurements within smoke plumes often showed clear enhancements in O₃ concentration above typical background levels. Examples are shown in Figure 1. The red shaded regions show increases in O₃ levels when smoke was monitored in the afternoon of February 11, 12, and 13, 2022 at Fort Moore. Focusing on just daytime periods between 12:00 and 18:00, when regional O₃ concentrations were elevated due to photochemical activity, O₃ enhancement above the general daily trend was observed in 31 out of 32 plumes (other smoke events identified are either fully or mostly captured outside this time frame). The 20 min average maximum ΔO₃ (peak O₃ – background O₃) for all daytime smoke events range from 5.1 to 134 ppb, where the upper concentrations are substantially higher than background levels (Table 1). (This range excludes event 11 on April 21, 2021, at Fort Moore, during which the fire was within 143 m of the trailer. As shown in the time series in Figure S6, this smoke event was detected before noon and continued until the next morning.)

For the 31 plumes in which O₃ was produced, O₃ NEMRs range between 5.32×10^{-3} and 0.143 ppb ppb⁻¹. While the overall coefficient of determination (r^2) for O₃ versus CO is low for all data combined, as shown in Figure 2d, due to the significant variability in the slope across different events (plumes), a strong correlation between O₃ and CO was observed within individual events, with r^2 values ranging from 0.49 to 1, (except for a fresh (5 min old) smoke event (number 37 in Table S1) resulting in an r^2 of 0.18). Lower coefficients of determination were usually encountered for longer duration

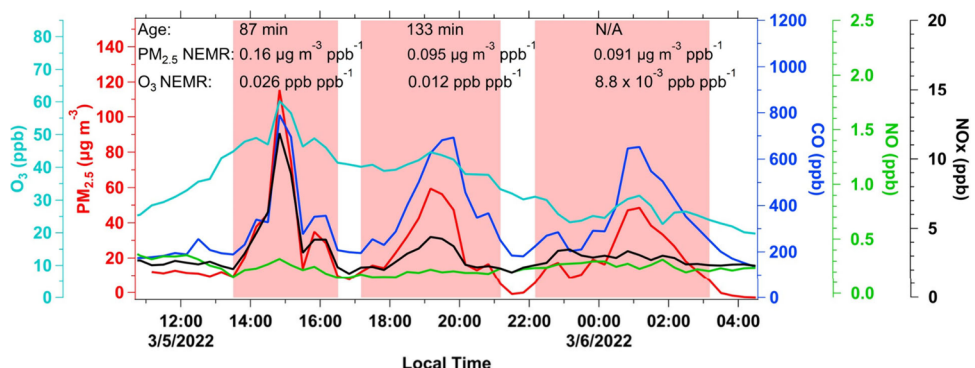


Figure 3. A time series showing a smoke event monitored during the day and night on March 5, 2022, at Fort Stewart. Time resolution is 20 min for CO , O_3 , NO , NO_x , and $\text{PM}_{2.5}$ mass. Red shaded areas correspond to smoke events from the same source and are identified by the covariability in CO and $\text{PM}_{2.5}$ mass.

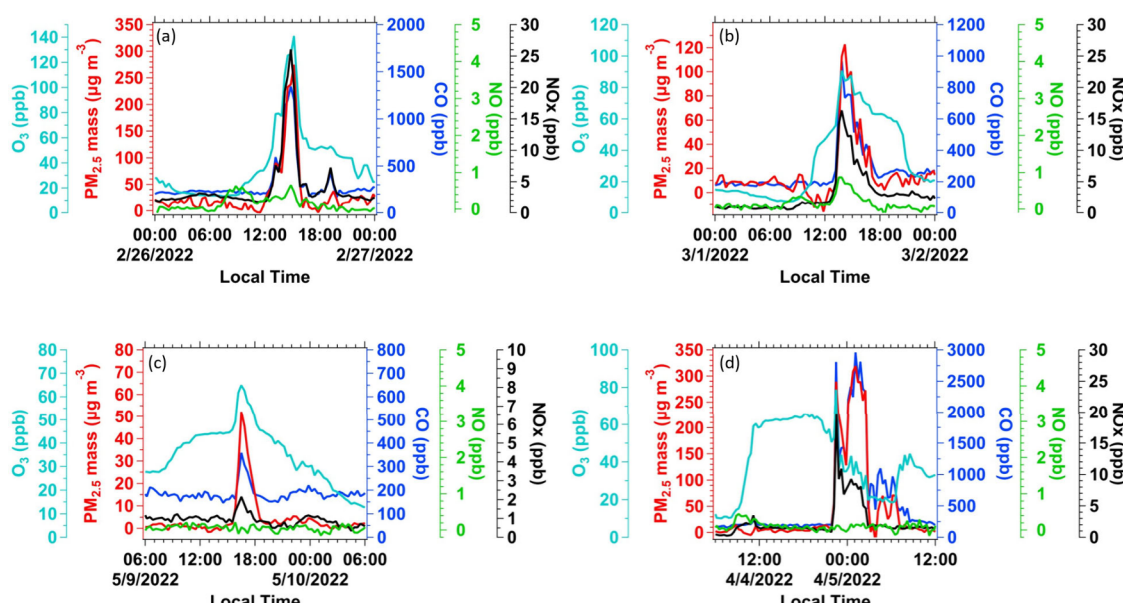


Figure 4. Time series showing the concentration of species measured at Fort Moore during 4 different smoke events. Measurement time resolution is 20 min for CO , $\text{PM}_{2.5}$ mass, O_3 , NO_x , and NO .

events due to complex photochemistry strongly affected by factors such as time of the day, wind conditions, and variation in emission, as discussed below.

In a few cases, O_3 enhancements were observed late in the evening and at night, likely due to O_3 from daytime fires persisting into these hours. Typically, nighttime O_3 to CO levels were lower relative to daytime values for smoke of similar age, with weak correlation and low coefficient of determination (r^2 reaches below 0.1), suggesting that some, but incomplete, O_3 loss within the plume had occurred. For example, the gray shaded region in Figure 1 shows smoke detected in the late evening and into the next morning. Based on wind data, this was smoke from the same source detected earlier in the day of February 13, 2022 (at 13:00 and then again after 18:00), as shown in Figure 1. On this day, the first peak started at 10:40 in the morning and continued until the afternoon. Another peak was observed after 18:00 and continued until the night and next day (note concentrations of CO , $\text{PM}_{2.5}$ mass, BC, and BrC). In this case, some enhancements in O_3 were seen, altering its diurnal profile and causing higher nighttime O_3 than usual. Similar behavior was

observed at other times at Fort Moore, as well as during the intensive study at Fort Stewart in 2022.

Another example is shown in Figure 3, where smoke from the same fire at Fort Stewart was measured at three different times at the same site due to wind variations. Clear O_3 enhancement is seen during the first peak, which was recorded during the day (14:30 to 15:30), then in the evening (19:00–20:00) and then during the night (1:00–2:00 the next day) where residual O_3 persisted, disrupting the typical nighttime O_3 levels (Figure S4). The O_3 NEMRs and O_3 - CO correlations progressively dropped with time of day and were 2.63×10^{-2} , 1.17×10^{-2} , and $8.85 \times 10^{-3} \text{ ppb ppb}^{-1}$, with corresponding r^2 values of 0.94, 0.46, and 0.21, respectively. This progression shows that O_3 NEMRs drop off when O_3 production ceases due to no photochemistry.

Influence of NO_x . We focus on the role of nitrogen oxides (NO_x) in the loss of O_3 and not O_3 production since we do not have VOC data. NO_x is produced in combustion processes and was clearly elevated during smoke events, as shown as an example in Figures 3 and 4. In general, NO_x in the plumes was correlated with CO ($r^2 = 0.87$ for combined data) during photochemically active periods (12:00–18:00) with NO_x

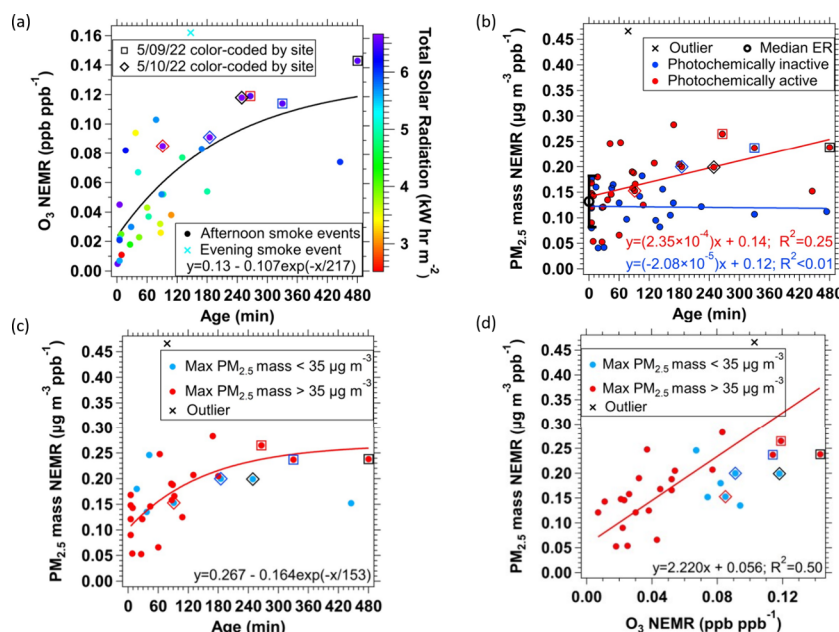


Figure 5. (a) O_3 NEMRs ($\Delta O_3/\Delta CO$) of all smoke events measured during the daytime (12:00 to 18:00) as a function of plume physical age and color coded by total solar radiation on the day of the event; (b) $PM_{2.5}$ mass NEMRs ($\Delta PM_{2.5}$ mass/ ΔCO) of all smoke events studied as a function of age. The median emission ratio (age less than 1 h) is shown in black with error bar as one standard deviation; (c) $PM_{2.5}$ mass NEMRs as a function of age of photochemically active smoke events (i.e., time of day between 12:00 and 18:00) for plumes where $PM_{2.5}$ mass concentration was less than or greater than $35 \mu g m^{-3}$; (d) Correlation between $PM_{2.5}$ mass NEMRs with O_3 NEMRs for all photochemically active smoke events based on $PM_{2.5}$ mass concentration; slopes are derived from orthogonal distance regression (ODR). As noted in (a), the diamond and square markers are data from plumes shown in Figure 6.

NEMRs (slopes of NO_x vs CO) ranging from 6.0×10^{-3} to 2.9×10^{-2} ppb ppb⁻¹. There was little correlation between NO_x and CO in the smoke plumes during photochemically inactive periods, 19:00–11:00 the next day. NO_x NEMRs was not correlated with O_3 or $PM_{2.5}$ mass NEMRs when comparing between plumes (Figure S7).

Figures 3 and 4 show that most of the NO_x was NO_2 , which is available for the formation of O_3 through NO_2 photolysis. O_3 production may occur throughout smoke plumes in prescribed fires where sunlight may more easily penetrate the plume, compared to large wildfires where light absorption may limit photochemistry within the interior of the plumes.²⁶ Once photochemistry stops, NO_x can lead to loss of O_3 (i.e., O_3 titration by $NO + O_3$ makes $NO_2 + O_2$), but this process slows in the aging plume since the NO is consumed and there are no significant NO sources (i.e., input from the fire and NO is not regenerated by NO_2 photolysis). As an example, in Figure 4, O_3 enhancements were observed in the afternoon (Figure 4a,b), late in the evening (Figure 4c), and near midnight (Figure 4d), and the prominent form of NO_x ($NO + NO_2$) was NO_2 ; NO_2/NO_x ratios for these four events are 0.97, 0.95, 1.0, and 0.99, respectively. The NO concentrations for these plumes were 0.657 and 0.871 ppb in Figure 4a and b, respectively, and below the LOD of 0.40 ppb in Figure 4c,d. This implies slow O_3 titration by NO . This was also observed in the three plumes from the same fire observed in the afternoon into the night as shown in Figure 3, where NO concentration was below LOD of 0.40 ppb for all three peaks. Decrease in atmospheric mixing as the boundary layer lowers at night may also have some effect on concentrations.

For all plumes (which is limited by available NO_x data), daytime NO levels ranged from below the LOD to 1.57 ppb, while in nighttime plumes, NO consistently remained below

LOD (0.40 ppb). From this, based on its reaction with NO (using $NO-O_3$ reaction rate constant of $1.8 \times 10^{-14} \text{ cm}^3 \text{ molecule}^{-1} \text{ s}^{-1}$),⁵³ the estimated O_3 lifetime ranged from 24 min to 4.5 h during the day, and from 2.2 to 8 h at night (lifetimes above 1.5 h are calculated from NO concentrations below our measurement LOD).

The residual O_3 and NO_2 at night suggest the formation of nitrate radical and associated chemistry can occur.^{54–56} Below we show that there is no observed net increase in $PM_{2.5}$ NEMRs at night suggesting that nighttime nitrate radical chemistry does not produce any enhancements in $PM_{2.5}$. Overall, we find that O_3 from smoke may at times affect nighttime O_3 concentrations, apparently, in part, due to low NO concentrations in the plumes.

$PM_{2.5}$ Mass Enhancement. Unlike O_3 that is not directly emitted, for $PM_{2.5}$ species, both primary emissions and secondary formation contribute to observed concentrations. Significant primary $PM_{2.5}$ emissions may explain why $PM_{2.5}$ mass concentration enhancements above the background levels were observed in all smoke plumes monitored at any time (day and night). $\Delta PM_{2.5}$ mass (peak $PM_{2.5}$ mass–background $PM_{2.5}$ mass) ranged between 17.1 to 839 $\mu g m^{-3}$. (This excludes the fresh smoke event 11 on April 21, 2021, Figure S6, which was close to the inlets causing a filter overload in particles after exceeding a 20 min $PM_{2.5}$ mass of 2000 $\mu g m^{-3}$). $PM_{2.5}$ mass NEMRs ($\Delta PM_{2.5}$ mass concentration/ ΔCO concentration) in this study ranged from 4.06×10^{-2} to $0.466 \mu g m^{-3}$ ppb⁻¹.

$PM_{2.5}$ Mass Emission Ratios from NEMRs of Fresh Smoke. Since $PM_{2.5}$ is directly emitted from fires (i.e., primary emissions), $PM_{2.5}$ emission ratios (ERs) in the studied smoke plumes were also determined. This was done by classifying all $PM_{2.5}$ NEMRs for plumes with an estimated ages of less than 1 h as an ER,⁴⁰ assuming minimal chemical and

physical evolution within this time. (This is not done for O_3 since it is secondary). In this study, $PM_{2.5}$ mass ERs median value was $0.132 \mu\text{g m}^{-3} \text{ ppb}^{-1}$ with IQR of 7.10×10^{-2} . No significant difference was observed in $PM_{2.5}$ emissions for fires at the different Forts; ERs from measurements at Fort Stewart in 2024, were 0.145 and $0.143 \mu\text{g m}^{-3} \text{ ppb}^{-1}$ for smoke reaching the two trailers in 4 and 9 min, respectively. The emissions from this study are similar to those reported for many other prescribed fires, but lower than what has been reported for wildfires (see El Asmar et al. for a detailed comparison).⁵¹

No significant difference (two-tailed p-value = 0.645) was observed between the ERs for smoke events measured at different times of the day, indicating that ERs are likely not affected by photochemical production. For example, ER detected between 9:00 and 17:00 had a mean ER of $0.129 \mu\text{g m}^{-3} \text{ ppb}^{-1}$ (median = 0.135), similar to smoke from fires detected late in the evening (after 17:00) or early in the following morning (before 9:00), which had a mean ER of $0.119 \mu\text{g m}^{-3} \text{ ppb}^{-1}$ (median = 0.129). Mean $PM_{2.5}$ mass ERs for smoke events with enhanced O_3 was $0.129 \mu\text{g m}^{-3} \text{ ppb}^{-1}$ (median = 0.135) and showed no deviation within the range of ERs recorded; combined, these results indicate that any potential secondary aerosol formation within the first hour after emissions (the criteria for calculating ERs) did not significantly contribute to variability in $PM_{2.5}$ mass NEMR.

3.4. Evolution of Ozone Enhancement in Prescribed Fire Plumes. *Change of O_3 Enhancement with Age.* We first assess how rapidly O_3 formation begins following emissions from the burning area. There were 8 cases where smoke was detected during the day and the smoke age was less than 10 min. In these cases, low but clear O_3 enhancement was observed in all events, where O_3 NEMRs ranged from 5.32×10^{-3} to $4.53 \times 10^{-2} \text{ ppb ppb}^{-1}$. This corresponded to distances of 143 to 1,660 m downwind from the fire. There was one exception (event number 68; the 1 out of 32 smoke events) on February 10, 2024, at Fort Stewart, where no O_3 enhancement was recorded when smoke was transported over 730 m in 4 min. Overall, we find that for daytime emissions, O_3 is produced very rapidly and near the fires.

For longer time scales (smoke ages), a trend in O_3 production as the plume ages was observed. As shown in Figure 5a, O_3 NEMR increased in smoke transported for periods up to about 480 min (8 h) with a moderate coefficient of determination between O_3 NEMR and smoke age ($r^2 = 0.53$). These data only include smoke recorded up to late in the evening (19:00) after which photochemistry ceases (Figure S4). An exponential fit shown in Figure 5a suggests that the rate of increase in O_3 is initially rapid, with the concentration doubling in the first ~ 53 min, after which it gradually levels off over time approaching an NEMR of $0.130 \text{ ppb ppb}^{-1}$ with an e-folding time of roughly 220 min (~ 3.5 h).

As a specific example, evolution of smoke from a single fire was also observed. These contrast with the ensemble of separate smoke plumes shown in Figure 5a. The time series of two smoke events detected sequentially at 3 monitoring trailers on May 9 and 10, 2022, is shown in Figure 6. On May 9, the peaks corresponding to the smoke from the same fire were monitored at 14:50, 16:30, and 17:50 (sampling trailers T 1291, T Main, and T 1293, respectively, see Figure S2) with estimated ages of 296, 330, and 480 min. Corresponding O_3 NEMRs determined from the slopes of ΔO_3 vs ΔCO (see Figure S8a) are 0.119, 0.114, and $0.143 \text{ ppb ppb}^{-1}$ in the same

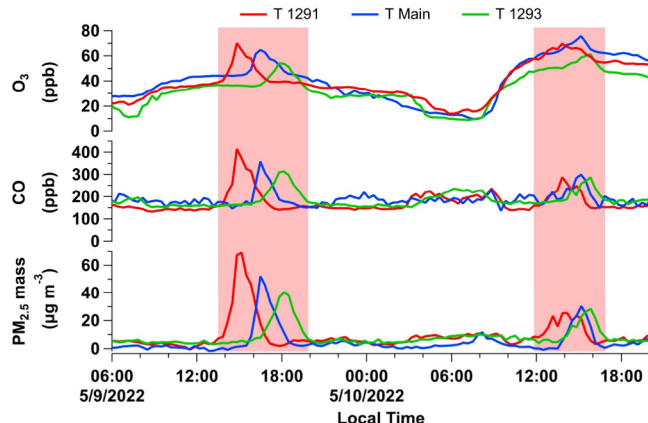


Figure 6. Time series showing two smoke events (red shaded regions) identified by the covariability in CO and $PM_{2.5}$ mass and detected sequentially at three monitoring trailers on May 9 and 10, 2022, at Fort Moore. Time resolution is 20 min for CO, O_3 , and $PM_{2.5}$ mass.

sequential order of the smoke reaching the trailers. There is no significant difference ($\sim 4\%$ decrease) in O_3 NEMRs between the first two trailers that measured O_3 peaks 40 min apart. However, an approximate 20% increase in O_3 NEMR is observed between the first and last locations, where the peaks were seen 180 min apart. In another case, also shown in Figure 6, on May 10, the peaks corresponding to one burning event were detected at 13:50, 15:10, and 15:50 (at T 1291, T Main, and T 1293 respectively) corresponding to plume ages of 91, 185, and 249 min. O_3 NEMRs increased sequentially (Figure S8b); 8.51×10^{-2} to 9.14×10^{-2} to $0.118 \text{ ppb ppb}^{-1}$. This reflects an increase of 7% in O_3 NEMR in 80 min and $\sim 39\%$ in 120 min. These case studies are also identified in Figure 5a, allowing comparison of smoke evolution from a single fire to the general trend observed for all different smoke plumes combined. The results show a trend, but there is scatter, especially in the more aged smoke where more factors could affect the results as the plumes age, such as changing radiation levels throughout the day.

3.5. $PM_{2.5}$ Evolution and Link to O_3 . We did a similar analysis for $PM_{2.5}$ mass and investigated linkages between formation of O_3 and $PM_{2.5}$ mass. For all data combined, $PM_{2.5}$ mass NEMRs varied between 4.06×10^{-2} and $4.66 \times 10^{-2} \mu\text{g m}^{-3} \text{ ppb}^{-1}$ and were variable as a function of age with a positive yet very small slope and low coefficient of determination indicating little trend with increasing plume age (regression fit: $PM_{2.5}$ mass NEMR = $(1.44 \times 10^{-3} \pm 6.3 \times 10^{-5} \mu\text{g m}^{-3} \text{ ppb}^{-1} \text{ min}^{-1}) \text{ Age} + 0.132 \mu\text{g m}^{-3} \text{ ppb}^{-1}$, $r^2 = 0.1$; Figure 5b). (Note that the intercept of $0.132 \mu\text{g m}^{-3} \text{ ppb}^{-1}$ is the same value as the median ER discussed above.) The data in Figure 5b are divided into periods; when O_3 enhancements were not observed (periods of little to no sunlight, e.g., evening, nighttime, or morning, Figure S4), and when O_3 enhancements were observed (i.e., photochemically active (12:00 to 18:00)). The largely nighttime smoke events, represented by blue markers in Figure 5b, show low coefficient of determination between $PM_{2.5}$ mass NEMRs and smoke age ($r^2 = 0.004$), with slope close to zero ($-2.08 \times 10^{-5} \mu\text{g m}^{-3} \text{ ppb}^{-1} \text{ min}^{-1}$). In contrast, considering only photochemically active periods, (daytime smoke plumes in which O_3 enhancements were observed), $PM_{2.5}$ mass NEMRs show a slight positive correlation with age with a higher coefficient of

determination ($r^2 = 0.25$), indicating that there might be secondary aerosol formation through a photochemical process. This coefficient of determination, however, was higher when considering only plumes of higher PM_{2.5} mass concentration ($r^2 = 0.43$; i.e., smoke plumes that have a 20 min average maximum PM_{2.5} mass concentration above 35 $\mu\text{g m}^{-3}$). This may result from the effect of evaporation of semivolatile species from PM_{2.5} in plumes that have lower PM_{2.5} mass concentrations. Assessing PM_{2.5} NEMRs versus time of day (Figure S11), we found higher NEMRs during the day. PM_{2.5} mass NEMR in smoke measured at night had magnitudes more similar to those seen within 1 h of emissions (i.e., ER of 0.132 $\pm 0.051 \mu\text{g m}^{-3} \text{ ppb}^{-1}$).

Like O₃ NEMRs vs age, the PM_{2.5} mass NEMRs for the higher concentration smoke plumes (greater than 35 $\mu\text{g m}^{-3}$) tend to also follow an exponential trend, as shown in Figure 5c. From the fit, the rate of increase in PM_{2.5} mass relative to CO is initially rapid, with the NEMR doubling in ~ 150 min and then gradually slowing down over time approaching 0.267 $\mu\text{g m}^{-3} \text{ ppb}^{-1}$. Thus, after approximately 150 min the amount of secondary aerosol mass relative to what was emitted is roughly equal ([0.267 $\mu\text{g m}^{-3} \text{ ppb}^{-1}$ – 0.132 $\mu\text{g m}^{-3} \text{ ppb}^{-1}$] / 0.132 $\mu\text{g m}^{-3} \text{ ppb}^{-1}$ = 1.02, where 0.132 $\mu\text{g m}^{-3} \text{ ppb}^{-1}$ is the ER), implying that after approximately 150 min, the PM_{2.5} mass NEMR had doubled relative to the ER. Overall, the trend in PM_{2.5} mass NEMRs is not as clear as that of O₃ NEMRs (Figure 5a), possibly reflecting the variability in primary PM_{2.5} and competing processes of secondary aerosol formation and loss by evaporation.

We also compare the PM_{2.5} mass NEMRs with age for evolution of single smoke plume recorded at different measurement sites, as done for the O₃ case study discussed above. The smoke events monitored sequentially on May 9, 2022, in Figure 6, corresponds to smoke of ages 266, 330, and 480 min. (Scatter plots of PM_{2.5} mass vs CO (slope = NEMR) are shown in Figure S8c,d.) These events are also specifically identified in Figure 5b–d. For these data, PM_{2.5} mass NEMRs are fairly constant and fall in the higher age region where the exponential trend flattens, suggesting secondary aerosol formation had slowed down or more nearly balanced by PM_{2.5} loss, with plume dilution, but variability in emissions cannot be ruled out. A similar result was observed for the other smoke plume measured the next day (5/10/2022 in Figure 6).

4. DISCUSSION

We observed enhancements in O₃ NEMR almost immediately after emissions (plumes of age estimated between 1 and 5 min) for smoke measured during the daytime. Some studies suggest that this may result from rapid radical formation through photolysis of HONO and HCHO,²³ while other studies (Figure S9), observed negative initial O₃ NEMRs due to background O₃ depletion through fast titration by freshly emitted NO.^{3,57,58}

Following rapid formation, we found that physical age had the greatest impact on the variation of O₃ NEMRs among different smoke plumes. O₃ NEMRs increased significantly as the estimated physical age of the smoke events ranged from a few minutes to 1–2 h, then continued to increase more slowly in events with estimated age up to 8 h, starting at $5.32 \times 10^{-3} \text{ ppb ppb}^{-1}$ in 1 min old smoke and reaching 0.143 ppb ppb⁻¹ in 8 h old plumes. The slowdown is likely due to decreasing photochemistry and O₃ formation as the end of the day approaches, as observed by Robinson et al.²² An exponential fit

of O₃ NEMRs vs time characterizes this process as the O₃ NEMR asymptotically reaches a constant value. These data can be compared to O₃ formation observed in other studies of different types of fires (see Figure S9). Changes of O₃ NEMRs with age observed in this study generally align with O₃ NEMRs up to about 2 h of aging observed for tropical, subtropical, and Alaskan wildfires,^{24,58–60} as well as for agricultural fires in the southeastern US.³ However, they differ from wildfires in the western US and Canada, which have lower O₃ NEMRs reported at similar ages.^{61,62} Comparison with similar types of prescribed fires in South Carolina (composed primarily of longleaf pine) for smoke up to 4.5 h old showed similarly rapid formation of O₃ and comparable O₃ NEMRs.¹⁷ Our measurement approach provided data on O₃ NEMR evolution over longer time periods than these studies (8 h). A more detailed comparison is provided in Supporting Information, Section S.1 (comparison of evolution of O₃ with other studies).

Along with O₃ production observed in the afternoon on clear days during the photochemically active periods, we also observed evidence for a net increase in PM_{2.5} mass NEMR as the plumes aged. PM_{2.5} mass and O₃ NEMRs for these aging plumes tended to be correlated, as shown in Figure 5d. For the plumes of higher PM_{2.5} mass concentration (>35 $\mu\text{g m}^{-3}$) the r^2 was 0.50, whereas for all the data the r^2 was 0.39. This likely reflects that photochemistry produced both secondary O₃ and aerosol.^{26,63–65} Both O₃ and PM_{2.5} mass NEMRs were observed to change more slowly with plume age (Figure 5a,c) but PM_{2.5} mass NEMR appears to drop off more relative to O₃ at higher ages (Figure 5d), which results in less correlation between O₃ and PM_{2.5} mass NEMRs. This may reflect evaporation of semivolatile aerosol species as the plumes dilute, with no similar process for O₃, along with possible additional differences in aging processes.

Our findings on PM_{2.5} evolution in prescribed fires differ from those of wildland and agricultural fires, as well as from some prescribed fires reported in other studies. For wildland fires with similar aging time scales as ours, PM_{2.5} mass NEMRs have time trends ranging from systematic increase,^{66–68} no change,^{68–70} to decrease⁶⁸ with smoke age. No systematic increase in OA NEMRs in plumes up to 1.2 h has been reported for agricultural fires in the southeastern US.³ For prescribed fires in the southeast, May et al. found no statistically significant change in OA NEMRs over 1.5 h of transport for two events in South Carolina that involved burning of forested lands composed primarily of longleaf pine.⁷¹ A decrease in OA NEMRs was observed over a longer period (2–5 h of transport)⁷¹ during a photochemically active period with observed O₃ formation,¹⁷ however, the plume had rapidly diluted ($\Delta\text{CO} \sim 25 \text{ ppb}$ after 1–1.5 h of aging) suggesting that evaporation might have dominated over OA formation. In contrast, we always observed an increase in PM_{2.5} mass NEMRs with age for the first 8 h following emissions during photochemically active periods. A more detailed comparison for PM_{2.5} mass NEMRs with other studies is provided by El Asmar et al. (2024).⁵¹ The increase in O₃ production and aerosol formation observed in our study in comparison with other types of fires could be attributed to the smoke being optically thinner relative to larger wildland and large agricultural fires, allowing more sunlight penetration into the plume and increased photochemical activity throughout the plume. Wildfire plumes are often much larger with higher OA concentrations^{72,73} and emission factors of PM_{2.5}⁷⁴ with

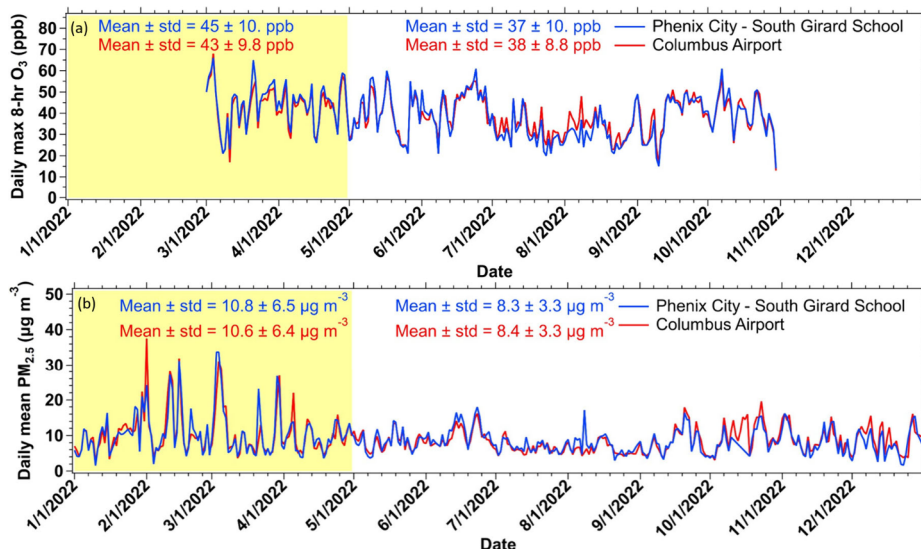


Figure 7. Data reported at two state sites, Columbus Airport and Phenix City South Girard School, showing (a) a daily maximum of 8 h O_3 in March through October of 2022 and (b) daily mean $PM_{2.5}$ concentration throughout the same year. The highlighted portion corresponds to the period of significant prescribed burning (January–April) in the southeastern US. Note that O_3 is not measured in the colder months.

high aerosol optical extinction at their darker centers, resulting in a reduced actinic flux and photolysis rates.²⁶

Unlike O_3 , secondary $PM_{2.5}$ can be formed at night through nighttime chemical processes that form both inorganic⁷⁵ and organic nitrogen species,^{75,76} enhanced by lower temperatures (reduce species volatility) and producing higher relative humidities (more particle liquid water) that promotes heterogeneous reactions.⁷⁷ As noted in Figure 3b, no increase in NEMRs with age was observed for photochemically inactive periods (night and early morning). During these times, $PM_{2.5}$ mass NEMRs were similar to estimated ER of $0.132 \mu\text{g m}^{-3} \text{ ppb}^{-1}$ and there was no evidence of any systematic change in $PM_{2.5}$ mass NEMRs with age.

The broader impact of prescribed burning on air quality, including cardiovascular and respiratory effects as well as mortality rates, beyond the immediate vicinity of the fires is a significant concern and has been investigated.^{78,79} It is complicated by many factors, such as the variability and evolution of emissions, changes in meteorology, photochemistry as the smoke is advected from the burning region, and the mixing of emissions from other sources, e.g., biogenic VOCs, NO_x from urban regions and other fires in the area (possibly with different fuels e.g., agricultural burning). The EPA National Emission Inventory estimates that in the southeastern US, the region including these measurements, roughly 30% of primary $PM_{2.5}$ in the winter is from prescribed burning.^{79,80} Northwest of Fort Moore are two state monitors that provide a larger context for O_3 and $PM_{2.5}$ mass (see site locations in map Figure S2). We note that burning also often occurs in regions around Fort Moore during the burning season⁵¹ so the impacts at these urban sites can be from fires throughout the region, beyond the Fort. The time series of daily maximum 8-h O_3 concentrations (i.e., what is reported by the state) and $PM_{2.5}$ mass concentration measured at these sites for 2022 are shown in Figure 7. The mean daily maximum 8-h O_3 concentrations at the two state sites were generally higher in March and April compared to other months, though not significantly higher in all cases. The mean O_3 during these months were 43 ppb (at Columbus Airport) and 45 ppb (at Phenix City South Girard School), while in other months, they

ranged from roughly 31 to 44 ppb at both sites (more data is given in Figure 7). Comparisons for both sites based on medians give similar results; the median O_3 in March and April were 44–48 ppb compared to 30–46 ppb in other months. Although the prescribed burning period spans from January to April, O_3 data is only available from March to October.

The difference in $PM_{2.5}$ mass concentration between burning season and the rest of the year is more pronounced with numerous peaks in both the daily (Figure 7b) and hourly (Figure S12) averaged $PM_{2.5}$ mass concentrations during the burning season. The daily mean $PM_{2.5}$ mass concentrations exceeded $20 \mu\text{g m}^{-3}$ multiple times at each site during the burning season but never during the rest of the year. Daily means of $PM_{2.5}$ mass concentration (shown in Figure 7) were 26 to 30% higher during the springtime burning period (see Figure 7b). Median $PM_{2.5}$ mass concentrations during the burning period (first four months of 2022) were $9.0 \mu\text{g m}^{-3}$ (IQR = 7.7) at Columbus Airport site and $9.6 \mu\text{g m}^{-3}$ (IQR = 5.5) at Phenix City South Girard School, whereas median $PM_{2.5}$ mass concentrations during the rest of the year, which were $7.7 \mu\text{g m}^{-3}$ (IQR = 4.6) and $7.8 \mu\text{g m}^{-3}$ (IQR = 4.3) at Columbus Airport and Phenix City South Girard School sites, respectively. The burn vs nonburn season differences in $PM_{2.5}$ mass are roughly 1.6 (based on medians) to 2.4 (based on means), which are roughly in the range of the approximate $1 \mu\text{g m}^{-3}$ increase based on modeling estimates for the southeast in general for years 2013–2020.⁷⁹

The contrast between observations at the state monitoring sites for O_3 and $PM_{2.5}$ is likely due to several factors. It is noteworthy that for the most aged plumes, $PM_{2.5}$ mass NEMRs are about a factor of 2 higher than that of O_3 (see Figure 5). Thus, as the plumes dilute into the background air, $PM_{2.5}$ mass has about twice the perturbation relative to background conditions. Aging processes further complicate things. NEMRs will likely continue to change as the plume is diluted, which will differ between $PM_{2.5}$ mass and O_3 . A significant fraction of $PM_{2.5}$ in smoke are primary particles, with the more variable addition of secondary species, as seen in this study. In contrast, O_3 is secondary and depends on many factors beyond just the emissions from the fires, such as solar radiation which increases

in summertime relative to the period of burning and seasonal changes in biogenic VOC emissions that are significant in this region.^{81,82} These data show a regional impact from prescribed burning, which is noteworthy given the possible health implications associated with PM_{2.5}.^{79,83} Smoke reaching these areas is often aged and as shown here, may contain secondary pollutants such as O₃ and secondary aerosols that could have especially harmful effects on human health.⁸⁴

5. CONCLUSION

This study analyzed smoke plumes from prescribed fires across multiple ground-based sites in the southeastern USA during the burning seasons of 2021 through 2024 to assess the formation and evolution of O₃ and PM_{2.5} mass. Data from 69 smoke events revealed rapid O₃ production above background levels in daytime plumes observed between 12:00–18:00 (32 of the 69 plumes), with O₃ production beginning within minutes following emissions. As plumes drifted from the fire (source), O₃ NEMRs ($\Delta O_3 / \Delta CO$) increased with plume age, ranging from 5.32 to 143 ppb ppm⁻¹ over ages from 1 to 480 min. The increase was rapid in the first hour, followed by a gradual slowing, approximating an exponential relationship between O₃ NEMR and smoke age. Our observations of O₃ NEMR evolution are consistent with studies on tropical, subtropical, and Alaskan wildfires,^{57–60} southeastern US agricultural fires,³ and prescribed fires in South Carolina,¹⁷ but contrast with lower values reported for wildfires in the western US and Canada.^{61,62}

PM_{2.5} mass concentrations also indicated aerosol production alongside O₃. In photochemically active plumes, with enhanced O₃, PM_{2.5} mass NEMRs ($\Delta PM_{2.5} \text{ mass} / \Delta CO$) rose with age, suggesting secondary aerosol formation in these smoke plumes linked to O₃ production. Stronger correlation between PM_{2.5} mass NEMRs and O₃ NEMRs was observed in plumes with higher PM_{2.5} mass concentrations (>35 $\mu\text{g m}^{-3}$), possibly due to less evaporation of semivolatile PM_{2.5} species. The consistent trend of increasing PM_{2.5} mass NEMRs in photochemically active plumes contrasts with other studies, which show highly variable PM mass NEMRs with age in both wildland and agricultural fires. Overall, O₃ NEMR trends were more pronounced than those of PM_{2.5} mass, potentially due to more complex factors affecting PM_{2.5}.

The broader impact of prescribed burning in the southeastern US was evident in PM_{2.5} mass and O₃ concentrations at two state air quality monitoring sites in an urban area near the burn zones. Daily average PM_{2.5} mass concentrations were approximately 25 to 30% higher, with notably higher extremes, during the burning season (January through April) compared to the rest of the year (nonburning seasons). However, there was less difference in daily maximum 8 h O₃ levels, which is consistent with PM_{2.5} mass NEMRs being about twice those of O₃ in the most aged smoke we detected. Further research on the formation of O₃ and PM_{2.5} mass in prescribed fires at other locations would help determine the broader applicability of these findings.

■ ASSOCIATED CONTENT

Data Availability Statement

The data are available in a publicly accessible repository on Zenodo at [10.5281/zenodo.11222295⁸⁵](https://zenodo.10.5281/zenodo.11222295) and [10.5281/zenodo.14648144⁸⁶](https://zenodo.10.5281/zenodo.14648144).

SI Supporting Information

The Supporting Information is available free of charge at <https://pubs.acs.org/doi/10.1021/acsestair.4c00231>.

Additional discussion comparing the evolution of O₃ with findings from other studies (Text S.1); Summary of smoke events studied (Table S1); Maps of study region and the location of trailers and state-operated sampling sites (Figures S1 and S2); Illustration on determining background O₃ (Figure S3) and the diurnal profile of O₃ on days with no smoke (Figure S4); Correlation between daytime O₃ concentrations on days with no smoke impact and the daily total solar radiation (Figure S5); Time series showing a direct hit of smoke from a prescribed fire close to the monitors (Figure S6); Correlation between NO_x and CO and between NO_x NEMRs with O₃ and PM_{2.5} mass NEMRs for smoke events at different monitoring times (Figure S7); Orthogonal regression of ΔO_3 vs ΔCO and $\Delta PM_{2.5}$ vs ΔCO for smoke events sequentially monitored on May 9 and 10, 2022 at Fort Moore (Figure S8); Comparison of O₃ evolution with findings from other studies (Figure S9); PM_{2.5} mass NEMRs as a function of smoke age and time of the day at which the peak occurred (Figures S10 and S11); Hourly PM_{2.5} concentration reported at two state-operated sites throughout 2022 (Figure S12) (PDF)

■ AUTHOR INFORMATION

Corresponding Author

Rodney J. Weber – School of Earth and Atmospheric Sciences, Georgia Institute of Technology, Atlanta, Georgia 30331, United States;  orcid.org/0000-0003-0765-8035; Email: rweber@eas.gatech.edu

Authors

Rime El Asmar – School of Earth and Atmospheric Sciences, Georgia Institute of Technology, Atlanta, Georgia 30331, United States;  orcid.org/0009-0000-8231-7498

Zongrun Li – School of Civil and Environmental Engineering, Georgia Institute of Technology, Atlanta, Georgia 30331, United States;  orcid.org/0000-0003-4907-146X

Haofei Yu – Department of Civil, Environmental and Construction Engineering, University of Central Florida, Orlando, Florida 32816, United States;  orcid.org/0002-7930-8934

Susan O'Neill – USDA Forest Service, Pacific Northwest Research Station, Seattle, Washington 98103, United States

David J. Tanner – School of Earth and Atmospheric Sciences, Georgia Institute of Technology, Atlanta, Georgia 30331, United States

L. Gregory Huey – School of Earth and Atmospheric Sciences, Georgia Institute of Technology, Atlanta, Georgia 30331, United States;  orcid.org/0000-0002-0518-7690

M. Talat Odman – School of Civil and Environmental Engineering, Georgia Institute of Technology, Atlanta, Georgia 30331, United States

Complete contact information is available at:

<https://pubs.acs.org/doi/10.1021/acsestair.4c00231>

Notes

The authors declare no competing financial interest.

ACKNOWLEDGMENTS

We thank the authorities at Fort Moore, Fort Stewart, and Eglin AFB for hosting the field studies, the land management team at Fort Moore for sharing details about the burns, and the team of facilitators at Fort Stewart and Eglin AFB for their support in enabling our presence and field installations. R.E.A., Z.L., D.J.T., L.G.H., M.T.O., and R.J.W. were supported by the United States Army Corps of Engineers Contract W912HQ-20-C-0019 funding the Strategic Environmental Research and Development Program (SERDP) Project RC20-1047. Part of H.Y.'s travel for participating in 2024 Fort Stewart campaign was funded by NSF Grant #1931871.

REFERENCES

- (1) Crutzen, P. J.; Andreae, M. O. Biomass Burning in the Tropics: Impact on Atmospheric Chemistry and Biogeochemical Cycles. *Science* (80-). **1990**, *250* (4988), 1669–1678.
- (2) Akagi, S. K.; Yokelson, R. J.; Wiedinmyer, C.; Alvarado, M. J.; Reid, J. S.; Karl, T.; Crounse, J. D.; Wennberg, P. O. Emission Factors for Open and Domestic Biomass Burning for Use in Atmospheric Models. *Atmos. Chem. Phys.* **2011**, *11* (9), 4039–4072.
- (3) Liu, X.; Zhang, Y.; Huey, L. G.; Yokelson, R. J.; Wang, Y.; Jimenez, J. L.; Campuzano-Jost, P.; Beyersdorf, A. J.; Blake, D. R.; Choi, Y.; St. Clair, J. M.; Crounse, J. D.; Day, D. A.; Diskin, G. S.; Fried, A.; Hall, S. R.; Hanisco, T. F.; King, L. E.; Meinardi, S.; Mikoviny, T.; Palm, B. B.; Peischl, J.; Perring, A. E.; Pollack, I. B.; Ryerson, T. B.; Sachse, G.; Schwarz, J. P.; Simpson, I. J.; Tanner, D. J.; Thornhill, K. L.; Ullmann, K.; Weber, R. J.; Wennberg, P. O.; Wisthaler, A.; Wolfe, G. M.; Ziembka, L. D. Agricultural Fires in the Southeastern U.S. during SEAC4RS: Emissions of Trace Gases and Particles and Evolution of Ozone, Reactive Nitrogen, and Organic Aerosol. *J. Geophys. Res. Atmos.* **2016**, *121* (12), 7383–7414.
- (4) May, A. A.; McMeeking, G. R.; Lee, T.; Taylor, J. W.; Craven, J. S.; Burling, I.; Sullivan, A. P.; Akagi, S.; Collett, J. L.; Flynn, M.; Coe, H.; Urbanski, S. P.; Seinfeld, J. H.; Yokelson, R. J.; Kreidenweis, S. M. Aerosol Emissions from Prescribed Fires in the United States: A Synthesis of Laboratory and Aircraft Measurements. *J. Geophys. Res. Atmos.* **2014**, *119* (20), 11,826–11,849.
- (5) Yee, L. D.; Kautzman, K. E.; Loza, C. L.; Schilling, K. A.; Coggon, M. M.; Chhabra, P. S.; Chan, M. N.; Chan, A. W. H.; Hersey, S. P.; Crounse, J. D.; Wennberg, P. O.; Flagan, R. C.; Seinfeld, J. H. Secondary Organic Aerosol Formation from Biomass Burning Intermediates: Phenol and Methoxyphenols. *Atmos. Chem. Phys.* **2013**, *13* (16), 8019–8043.
- (6) Lim, C. Y.; Hagan, D. H.; Coggon, M. M.; Koss, A. R.; Sekimoto, K.; de Gouw, J.; Warneke, C.; Cappa, C. D.; Kroll, J. H. Secondary Organic Aerosol Formation from the Laboratory Oxidation of Biomass Burning Emissions. *Atmos. Chem. Phys.* **2019**, *19* (19), 12797–12809.
- (7) Mueller, S. E.; Thode, A. E.; Margolis, E. Q.; Yocom, L. L.; Young, J. D.; Iniguez, J. M. Climate Relationships with Increasing Wildfire in the Southwestern US from 1984 to 2015. *For. Ecol. Manage.* **2020**, *460*, No. 117861.
- (8) Westerling, A. L.; Hidalgo, H. G.; Cayan, D. R.; Swetnam, T. W. Warming and Earlier Spring Increase Western U.S. Forest Wildfire Activity. *Science* (80-). **2006**, *313* (5789), 940–943.
- (9) Stephens, S. L.; Agee, J. K.; Fulé, P. Z.; North, M. P.; Romme, W. H.; Swetnam, T. W.; Turner, M. G. Managing Forests and Fire in Changing Climates. *Science* **2013**, *342* (6154), 41–42.
- (10) Keane, R. E.; Karau, E. Evaluating the Ecological Benefits of Wildfire by Integrating Fire and Ecosystem Simulation Models. *Ecol. Modell.* **2010**, *221* (8), 1162–1172.
- (11) Kolden, C. We're Not Doing Enough Prescribed Fire in the Western United States to Mitigate Wildfire Risk. *Fire* **2019**, *2* (2), 30.
- (12) Ryan, K. C.; Knapp, E. E.; Varner, J. M. Prescribed Fire in North American Forests and Woodlands: History, Current Practice, and Challenges. *Front. Ecol. Environ.* **2013**, *11* (s1), e15–e24.
- (13) Haines, T. K.; Busby, R. L.; Cleaves, D. A. Prescribed Burning in the South: Trends, Purpose, and Barriers. *South. J. Appl. For.* **2001**, *25* (4), 149–153.
- (14) Kupfer, J. A.; Terando, A. J.; Gao, P.; Teske, C.; Hiers, J. K. Climate Change Projected to Reduce Prescribed Burning Opportunities in the South-Eastern United States. *Int. J. Wildl. Fire* **2020**, *29* (9), 764.
- (15) Addington, R. N.; Hudson, S. J.; Hiers, J. K.; Hurteau, M. D.; Hutcherson, T. F.; Matusick, G.; Parker, J. M. Relationships among Wildfire, Prescribed Fire, and Drought in a Fire-Prone Landscape in the South-Eastern United States. *Int. J. Wildl. Fire* **2015**, *24* (6), 778.
- (16) Hunter, M. E.; Robles, M. D. Tamm Review: The Effects of Prescribed Fire on Wildfire Regimes and Impacts: A Framework for Comparison. *For. Ecol. Manage.* **2020**, *475*, No. 118435.
- (17) Akagi, S. K.; Yokelson, R. J.; Burling, I. R.; Meinardi, S.; Simpson, I.; Blake, D. R.; McMeeking, G. R.; Sullivan, A.; Lee, T.; Kreidenweis, S.; Urbanski, S.; Reardon, J.; Griffith, D. W. T.; Johnson, T. J.; Weise, D. R. Measurements of Reactive Trace Gases and Variable O₃ & Lt;Sub&gt;3&Lt;/Sub&gt; Formation Rates in Some South Carolina Biomass Burning Plumes. *Atmos. Chem. Phys.* **2013**, *13* (3), 1141–1165.
- (18) Yokelson, R. J.; Burling, I. R.; Gilman, J. B.; Warneke, C.; Stockwell, C. E.; De Gouw, J.; Akagi, S. K.; Urbanski, S. P.; Veres, P.; Roberts, J. M.; Kuster, W. C.; Reardon, J.; Griffith, D. W. T.; Johnson, T. J.; Hosseini, S.; Miller, J. W.; Cocker, D. R.; Jung, H.; Weise, D. R. Coupling Field and Laboratory Measurements to Estimate the Emission Factors of Identified and Unidentified Trace Gases for Prescribed Fires. *Atmos. Chem. Phys.* **2013**, *13* (1), 89–116.
- (19) Burling, I. R.; Yokelson, R. J.; Akagi, S. K.; Urbanski, S. P.; Wold, C. E.; Griffith, D. W. T.; Johnson, T. J.; Reardon, J.; Weise, D. R. Airborne and Ground-Based Measurements of the Trace Gases and Particles Emitted by Prescribed Fires in the United States. *Atmos. Chem. Phys.* **2011**, *11* (23), 12197–12216.
- (20) Chameides, W. L. The Photochemical Role of Tropospheric Nitrogen Oxides. *Geophys. Res. Lett.* **1978**, *5* (1), 17–20.
- (21) Liu, S. C.; Kley, D.; McFarland, M.; Mahlman, J. D.; Levy, H. On the Origin of Tropospheric Ozone. *J. Geophys. Res. Ocean.* **1980**, *85* (C12), 7546–7552.
- (22) Robinson, M. A.; Decker, Z. C. J.; Barsanti, K. C.; Coggon, M. M.; Flocke, F. M.; Franchin, A.; Fredrickson, C. D.; Gilman, J. B.; Gkatzelis, G. I.; Holmes, C. D.; Lamplugh, A.; Lavi, A.; Middlebrook, A. M.; Montzka, D. M.; Palm, B. B.; Peischl, J.; Pierce, B.; Schwantes, R. H.; Sekimoto, K.; Selimovic, V.; Tyndall, G. S.; Thornton, J. A.; Van Rooy, P.; Warneke, C.; Weinheimer, A. J.; Brown, S. S. Variability and Time of Day Dependence of Ozone Photochemistry in Western Wildfire Plumes. *Environ. Sci. Technol.* **2021**, *55* (15), 10280–10290.
- (23) Lee, H.; Jaffe, D. A. Wildfire Impacts on O₃ in the Continental United States Using PM 2.5 and a Generalized Additive Model (2018–2023). *Environ. Sci. Technol.* **2024**, *58* (33), 14764–14774.
- (24) Jaffe, D. A.; Wigder, N. L. Ozone Production from Wildfires: A Critical Review. *Atmos. Environ.* **2012**, *51*, 1–10.
- (25) Ninneman, M.; Jaffe, D. A. The Impact of Wildfire Smoke on Ozone Production in an Urban Area: Insights from Field Observations and Photochemical Box Modeling. *Atmos. Environ.* **2021**, *267*, No. 118764.
- (26) Xu, L.; Crounse, J. D.; Vasquez, K. T.; Allen, H.; Wennberg, P. O.; Bourgeois, I.; Brown, S. S.; Campuzano-Jost, P.; Coggon, M. M.; Crawford, J. H.; DiGangi, J. P.; Diskin, G. S.; Fried, A.; Gargulinski, E. M.; Gilman, J. B.; Gkatzelis, G. I.; Guo, H.; Hair, J. W.; Hall, S. R.; Halliday, H. A.; Hanisco, T. F.; Hannun, R. A.; Holmes, C. D.; Huey, L. G.; Jimenez, J. L.; Lamplugh, A.; Lee, Y. R.; Liao, J.; Lindaas, J.; Neuman, J. A.; Nowak, J. B.; Peischl, J.; Peterson, D. A.; Piel, F.; Richter, D.; Rickly, P. S.; Robinson, M. A.; Rollins, A. W.; Ryerson, T. B.; Sekimoto, K.; Selimovic, V.; Shingler, T.; Soja, A. J.; St. Clair, J. M.; Tanner, D. J.; Ullmann, K.; Veres, P. R.; Walega, J.; Warneke, C.; Washenfelder, R. A.; Weibring, P.; Wisthaler, A.; Wolfe, G. M.; Womack, C. C.; Yokelson, R. J. Ozone Chemistry in Western U.S. Wildfire Plumes. *Sci. Adv.* **2021**, *7* (50), No. eabl3648.

- (27) Jaffe, D. A.; Schnieder, B.; Inouye, D. Technical Note: Use of PM 2.5 to CO Ratio as an Indicator of Wildfire Smoke in Urban Areas. *Atmos. Chem. Phys.* **2022**, *22* (18), 12695–12704.
- (28) Shrestha, B.; Brotzge, J. A.; Wang, J. Observations and Impacts of Long-Range Transported Wildfire Smoke on Air Quality Across New York State During July 2021. *Geophys. Res. Lett.* **2022**, *49* (19), No. e2022GL100216.
- (29) Phairuang, W.; Chetiyankornkul, T.; Suriyawong, P.; Amin, M.; Hata, M.; Furuchi, M.; Yamazaki, M.; Gotoh, N.; Furusho, H.; Yurtsever, A.; Watanabe, S.; Sun, L. Characterizing Chemical, Environmental, and Stimulated Subcellular Physical Characteristics of Size-Fractionated PMs Down to PM 0.1. *Environ. Sci. Technol.* **2024**, *58* (28), 12368–12378.
- (30) Bali, K.; Banerji, S.; Campbell, J. R.; Bhakta, A. V.; Chen, L.-W. A.; Holmes, C. D.; Mao, J. Measurements of Brown Carbon and Its Optical Properties from Boreal Forest Fires in Alaska Summer. *Atmos. Environ.* **2024**, *324*, No. 120436.
- (31) Golovushkin, N. A.; Kuznetsova, I. N.; Konovalov, I. B.; Nahaev, M. I.; Kozlov, V. S.; Beekmann, M. Analysis of Brown Carbon Content and Evolution in Smokes from Siberian Forest Fires Using AERONET Measurements. *Atmos. Ocean. Opt.* **2020**, *33* (3), 267–273.
- (32) Phairuang, W.; Chetiyankornkul, T.; Suriyawong, P.; Ho, S.; Paluang, P.; Furuchi, M.; Amin, M.; Hata, M. Daytime-Nighttime Variations in the Concentration of PM0.1 Carbonaceous Particles during a Biomass Fire Episode in Chiang Mai, Thailand. *Particuology* **2024**, *87*, 316–324.
- (33) Ito, A.; Myriokefalitakis, S.; Kanakidou, M.; Mahowald, N. M.; Scanza, R. A.; Hamilton, D. S.; Baker, A. R.; Jickells, T.; Sarin, M.; Bikkina, S.; Gao, Y.; Shelley, R. U.; Buck, C. S.; Landing, W. M.; Bowie, A. R.; Perron, M. M. G.; Guieu, C.; Meskhidze, N.; Johnson, M. S.; Feng, Y.; Kok, J. F.; Nenes, A.; Duce, R. A. Pyrogenic Iron: The Missing Link to High Iron Solubility in Aerosols. *Sci. Adv.* **2019**, *5* (5), No. eaau7671.
- (34) Oakes, M.; Rastogi, N.; Majestic, B. J.; Shafer, M.; Schauer, J. J.; Edgerton, E. S.; Weber, R. J. Characterization of Soluble Iron in Urban Aerosols Using Near-real Time Data. *J. Geophys. Res. Atmos.* **2010**, *115* (D15), No. D15302.
- (35) Selimovic, V.; Yokelson, R. J.; McMeeking, G. R.; Coefield, S. Aerosol Mass and Optical Properties, Smoke Influence on O₃, and High NO₃ Production Rates in a Western U.S. City Impacted by Wildfires. *J. Geophys. Res. Atmos.* **2020**, *125* (16), No. e2020JD032791.
- (36) Lippmann, M. Health Effects of Tropospheric Ozone. *Environ. Sci. Technol.* **1991**, *25* (12), 1954–1962.
- (37) McConnell, R.; Berhane, K.; Gilliland, F.; London, S. J.; Islam, T.; Gauderman, W. J.; Avol, E.; Margolis, H. G.; Peters, J. M. Asthma in Exercising Children Exposed to Ozone: A Cohort Study. *Lancet* **2002**, *359* (9304), 386–391.
- (38) Manisalidis, I.; Stavropoulou, E.; Stavropoulos, A.; Bezirtzoglou, E. Environmental and Health Impacts of Air Pollution: A Review. *Front. Public Heal.* **2020**, *8*, 1–13.
- (39) Lippmann, M. OZONE. In *Environmental Toxicants*; Wiley, 2020; pp 783–853. DOI: [10.1002/9781119438922.ch21](https://doi.org/10.1002/9781119438922.ch21).
- (40) Cohen, A. J.; Brauer, M.; Burnett, R.; Anderson, H. R.; Frostad, J.; Estep, K.; Balakrishnan, K.; Brunekreef, B.; Dandona, L.; Dandona, R.; Feigin, V.; Freedman, G.; Hubbell, B.; Jobling, A.; Kan, H.; Knibbs, L.; Liu, Y.; Martin, R.; Morawska, L.; Pope, C. A.; Shin, H.; Straif, K.; Shaddick, G.; Thomas, M.; van Dingenen, R.; van Donkelaar, A.; Vos, T.; Murray, C. J. L.; Forouzanfar, M. H. Estimates and 25-Year Trends of the Global Burden of Disease Attributable to Ambient Air Pollution: An Analysis of Data from the Global Burden of Diseases Study 2015. *Lancet* **2017**, *389* (10082), 1907–1918.
- (41) Pardo, M.; Li, C.; He, Q.; Levin-Zaidman, S.; Tsoory, M.; Yu, Q.; Wang, X.; Rudich, Y. Mechanisms of Lung Toxicity Induced by Biomass Burning Aerosols. *Part. Fibre Toxicol.* **2020**, *17* (1), 4.
- (42) Reid, C. E.; Brauer, M.; Johnston, F. H.; Jerrett, M.; Balmes, J. R.; Elliott, C. T. Critical Review of Health Impacts of Wildfire Smoke Exposure. *Environ. Health Perspect.* **2016**, *124* (9), 1334–1343.
- (43) Garcia, A.; Santa-Helena, E.; De Falco, A.; de Paula Ribeiro, J.; Gioda, A.; Gioda, C. R. Toxicological Effects of Fine Particulate Matter (PM2.5): Health Risks and Associated Systemic Injuries—Systematic Review. *Water, Air, Soil Pollut.* **2023**, *234* (6), 346.
- (44) Xi, Y.; Kshirsagar, A. V.; Wade, T. J.; Richardson, D. B.; Brookhart, M. A.; Wyatt, L.; Rappold, A. G. Mortality in US Hemodialysis Patients Following Exposure to Wildfire Smoke. *J. Am. Soc. Nephrol.* **2020**, *31* (8), 1824–1835.
- (45) He, L.; Weschler, C. J.; Morrison, G.; Li, F.; Zhang, Y.; Bergin, M. H.; Black, M.; Zhang, J. J. Synergistic Effects of Ozone Reaction Products and Fine Particulate Matter on Respiratory Pathophysiology in Children with Asthma. *ACS ES&T Air* **2024**, *1* (8), 918–926.
- (46) Liu, C.; Chen, R.; Sera, F.; Vicedo-Cabrera, A. M.; Guo, Y.; Tong, S.; Lavigne, E.; Correa, P. M.; Ortega, N. V.; Achilleos, S.; Roye, D.; Jaakkola, J. J.; Rytí, N.; Pascal, M.; Schneider, A.; Breitner, S.; Entezari, A.; Mayvaneh, F.; Raz, R.; Honda, Y.; Hashizume, M.; Ng, C. F. S.; Gaio, V.; Madureira, J.; Holobaca, I.-H.; Tobias, A.; Íñiguez, C.; Guo, Y. L.; Pan, S.-C.; Masselot, P.; Bell, M. L.; Zanobetti, A.; Schwartz, J.; Gasparrini, A.; Kan, H. Interactive Effects of Ambient Fine Particulate Matter and Ozone on Daily Mortality in 372 Cities: Two Stage Time Series Analysis. *BMJ* **2023**, No. e075203.
- (47) Wong, J. P. S.; Tsagkaraki, M.; Tsiodra, I.; Mihalopoulos, N.; Violaki, K.; Kanakidou, M.; Sciaire, J.; Nenes, A.; Weber, R. J. Effects of Atmospheric Processing on the Oxidative Potential of Biomass Burning Organic Aerosols. *Environ. Sci. Technol.* **2019**, *53* (12), 6747–6756.
- (48) Liu, F.; Joo, T.; Ditto, J. C.; Saavedra, M. G.; Takeuchi, M.; Boris, A. J.; Yang, Y.; Weber, R. J.; Dillner, A. M.; Gentner, D. R.; Ng, N. L. Oxidized and Unsaturated: Key Organic Aerosol Traits Associated with Cellular Reactive Oxygen Species Production in the Southeastern United States. *Environ. Sci. Technol.* **2023**, *57* (38), 14150–14161.
- (49) Chowdhury, P. H.; He, Q.; Lasitza Male, T.; Brune, W. H.; Rudich, Y.; Pardo, M. Exposure of Lung Epithelial Cells to Photochemically Aged Secondary Organic Aerosol Shows Increased Toxic Effects. *Environ. Sci. Technol. Lett.* **2018**, *5* (7), 424–430.
- (50) Wang, S.; Gallimore, P. J.; Liu-Kang, C.; Yeung, K.; Campbell, S. J.; Uttinger, B.; Liu, T.; Peng, H.; Kalberer, M.; Chan, A. W. H.; Abbatt, J. P. D. Dynamic Wood Smoke Aerosol Toxicity during Oxidative Atmospheric Aging. *Environ. Sci. Technol.* **2023**, *57* (3), 1246–1256.
- (51) El Asmar, R.; Li, Z.; Tanner, D. J.; Hu, Y.; O'Neill, S.; Huey, L. G.; Odman, M. T.; Weber, R. J. A Multi-Site Passive Approach to Studying the Emissions and Evolution of Smoke from Prescribed Fires. *Atmos. Chem. Phys.* **2024**, *24* (22), 12749–12773.
- (52) Forrister, H.; Liu, J.; Scheuer, E.; Dibb, J.; Ziema, L.; Thornhill, K. L.; Anderson, B.; Diskin, G.; Perring, A. E.; Schwarz, J. P.; Campuzano-Jost, P.; Day, D. A.; Palm, B. B.; Jimenez, J. L.; Nenes, A.; Weber, R. J. Evolution of Brown Carbon in Wildfire Plumes. *Geophys. Res. Lett.* **2015**, *42* (11), 4623–4630.
- (53) Seinfeld, J. H.; Pandis, S. N. *Atmospheric Chemistry and Physics: From Air Pollution to Climate Change*, 3rd ed.; John Wiley & Sons, Inc., 2016.
- (54) Decker, Z. C. J.; Robinson, M. A.; Barsanti, K. C.; Bourgeois, I.; Coggon, M. M.; DiGangi, J. P.; Diskin, G. S.; Flocke, F. M.; Franchin, A.; Fredrickson, C. D.; Gkatzelis, G. I.; Hall, S. R.; Halliday, H.; Holmes, C. D.; Huey, L. G.; Lee, Y. R.; Lindaas, J.; Middlebrook, A. M.; Montzka, D. D.; Moore, R.; Neuman, J. A.; Nowak, J. B.; Palm, B. B.; Peischl, J.; Piel, F.; Rickly, P. S.; Rollins, A. W.; Ryerson, T. B.; Schwantes, R. H.; Sekimoto, K.; Thornhill, L.; Thornton, J. A.; Tyndall, G. S.; Ullmann, K.; Van Rooy, P.; Veres, P. R.; Warneke, C.; Washenfelder, R. A.; Weinheimer, A. J.; Wiggins, E.; Winstead, E.; Wisthaler, A.; Womack, C.; Brown, S. S. Nighttime and Daytime Dark Oxidation Chemistry in Wildfire Plumes: An Observation and Model Analysis of FIREX-AQ Aircraft Data. *Atmos. Chem. Phys.* **2021**, *21* (21), 16293–16317.
- (55) Brown, S. S.; Stutz, J. Nighttime Radical Observations and Chemistry. *Chem. Soc. Rev.* **2012**, *41* (19), 6405.

- (56) Ng, N. L.; Brown, S. S.; Archibald, A. T.; Atlas, E.; Cohen, R. C.; Crowley, J. N.; Day, D. A.; Donahue, N. M.; Fry, J. L.; Fuchs, H.; Griffin, R. J.; Guzman, M. I.; Herrmann, H.; Hodzic, A.; Inuma, Y.; Jimenez, J. L.; Kiendler-Scharr, A.; Lee, B. H.; Luecken, D. J.; Mao, J.; McLaren, R.; Mutzel, A.; Osthoff, H. D.; Ouyang, B.; Picquet-Varrault, B.; Platt, U.; Pye, H. O. T.; Rudich, Y.; Schwantes, R. H.; Shiraiwa, M.; Stutz, J.; Thornton, J. A.; Tilgner, A.; Williams, B. J.; Zaveri, R. A. Nitrate Radicals and Biogenic Volatile Organic Compounds: Oxidation, Mechanisms, and Organic Aerosol. *Atmos. Chem. Phys.* **2017**, *17* (3), 2103–2162.
- (57) Hobbs, P. V.; Sinha, P.; Yokelson, R. J.; Christian, T. J.; Blake, D. R.; Gao, S.; Kirchstetter, T. W.; Novakov, T.; Pilewskie, P. Evolution of Gases and Particles from a Savanna Fire in South Africa. *J. Geophys. Res. Atmos.* **2003**, *108* (D13), 8485.
- (58) Yokelson, R. J.; Bertschi, I. T.; Christian, T. J.; Hobbs, P. V.; Ward, D. E.; Hao, W. M. Trace Gas Measurements in Nascent, Aged, and Cloud-processed Smoke from African Savanna Fires by Airborne Fourier Transform Infrared Spectroscopy (AFTIR). *J. Geophys. Res. Atmos.* **2003**, *108* (D13), 8478.
- (59) Goode, J. G.; Yokelson, R. J.; Ward, D. E.; Susott, R. A.; Babbitt, R. E.; Davies, M. A.; Hao, W. M. Measurements of Excess O₃, CO₂, CO, CH₄, C₂H₄, C₂H₂, HCN, NO, NH₃, HCOOH, CH₃COOH, HCHO, and CH₃OH in 1997 Alaskan Biomass Burning Plumes by Airborne Fourier Transform Infrared Spectroscopy (AFTIR). *J. Geophys. Res. Atmos.* **2000**, *105* (D17), 22147–22166.
- (60) Yokelson, R. J.; Crounse, J. D.; DeCarlo, P. F.; Karl, T.; Urbanski, S.; Atlas, E.; Campos, T.; Shinozuka, Y.; Kapustin, V.; Clarke, A. D.; Weinheimer, A.; Knapp, D. J.; Montzka, D. D.; Holloway, J.; Weibring, P.; Flocke, F.; Zheng, W.; Toohey, D.; Wennberg, P. O.; Wiedinmyer, C.; Mauldin, L.; Fried, A.; Richter, D.; Walega, J.; Jimenez, J. L.; Adachi, K.; Buseck, P. R.; Hall, S. R.; Shetter, R. Emissions from Biomass Burning in the Yucatan. *Atmos. Chem. Phys.* **2009**, *9* (15), 5785–5812.
- (61) Liu, X.; Huey, L. G.; Yokelson, R. J.; Selimovic, V.; Simpson, I. J.; Müller, M.; Jimenez, J. L.; Campuzano-Jost, P.; Beyersdorf, A. J.; Blake, D. R.; Butterfield, Z.; Choi, Y.; Crounse, J. D.; Day, D. A.; Diskin, G. S.; Dubey, M. K.; Fortner, E.; Hanisco, T. F.; Hu, W.; King, L. E.; Kleinman, L.; Meinardi, S.; Mikoviny, T.; Onasch, T. B.; Palm, B. B.; Peischl, J.; Pollack, I. B.; Ryerson, T. B.; Sachse, G. W.; Sedlacek, A. J.; Shilling, J. E.; Springston, S.; St. Clair, J. M.; Tanner, D. J.; Teng, A. P.; Wennberg, P. O.; Wisthaler, A.; Wolfe, G. M. Airborne Measurements of Western U.S. Wildfire Emissions: Comparison with Prescribed Burning and Air Quality Implications. *J. Geophys. Res. Atmos.* **2017**, *122* (11), 6108–6129.
- (62) Alvarado, M. J.; Logan, J. A.; Mao, J.; Apel, E.; Riener, D.; Blake, D.; Cohen, R. C.; Min, K.-E.; Perring, A. E.; Browne, E. C.; Wooldridge, P. J.; Diskin, G. S.; Sachse, G. W.; Fuelberg, H.; Sessions, W. R.; Harrigan, D. L.; Huey, G.; Liao, J.; Case-Hanks, A.; Jimenez, J. L.; Cubison, M. J.; Vay, S. A.; Weinheimer, A. J.; Knapp, D. J.; Montzka, D. D.; Flocke, F. M.; Pollack, I. B.; Wennberg, P. O.; Kurten, A.; Crounse, J.; Clair, J. M. St.; Wisthaler, A.; Mikoviny, T.; Yantosca, R. M.; Carouge, C. C.; Le Sager, P. Nitrogen Oxides and PAN in Plumes from Boreal Fires during ARCTAS-B and Their Impact on Ozone: An Integrated Analysis of Aircraft and Satellite Observations. *Atmos. Chem. Phys.* **2010**, *10* (20), 9739–9760.
- (63) Murphy, S. M.; Sorooshian, A.; Kroll, J. H.; Ng, N. L.; Chhabra, P.; Tong, C.; Surratt, J. D.; Knipping, E.; Flagan, R. C.; Seinfeld, J. H. Secondary Aerosol Formation from Atmospheric Reactions of Aliphatic Amines. *Atmos. Chem. Phys.* **2007**, *7* (9), 2313–2337.
- (64) Alvarado, M. J.; Lonsdale, C. R.; Yokelson, R. J.; Akagi, S. K.; Coe, H.; Craven, J. S.; Fischer, E. V.; McMeeking, G. R.; Seinfeld, J. H.; Soni, T.; Taylor, J. W.; Weise, D. R.; Wold, C. E. Investigating the Links between Ozone and Organic Aerosol Chemistry in a Biomass Burning Plume from a Prescribed Fire in California Chaparral. *Atmos. Chem. Phys.* **2015**, *15* (12), 6667–6688.
- (65) Alvarado, M. J.; Prinn, R. G. Formation of Ozone and Growth of Aerosols in Young Smoke Plumes from Biomass Burning: 1. Lagrangian Parcel Studies. *J. Geophys. Res. Atmos.* **2009**, *114* (D9), No. D09306.
- (66) Pagonis, D.; Selimovic, V.; Campuzano-Jost, P.; Guo, H.; Day, D. A.; Schueneman, M. K.; Nault, B. A.; Coggon, M. M.; DiGangi, J. P.; Diskin, G. S.; Fortner, E. C.; Gargulinski, E. M.; Gkatzelis, G. I.; Hair, J. W.; Herndon, S. C.; Holmes, C. D.; Katich, J. M.; Nowak, J. B.; Perring, A. E.; Saide, P.; Shingler, T. J.; Soja, A. J.; Thapa, L. H.; Warneke, C.; Wiggins, E. B.; Wisthaler, A.; Yacovitch, T. I.; Yokelson, R. J.; Jimenez, J. L. Impact of Biomass Burning Organic Aerosol Volatility on Smoke Concentrations Downwind of Fires. *Environ. Sci. Technol.* **2023**, *57* (44), 17011–17021.
- (67) Gkatzelis, G. I.; Coggon, M. M.; Stockwell, C. E.; Hornbrook, R. S.; Allen, H.; Apel, E. C.; Bela, M. M.; Blake, D. R.; Bourgeois, I.; Brown, S. S.; Campuzano-Jost, P.; St. Clair, J. M.; Crawford, J. H.; Crounse, J. D.; Day, D. A.; DiGangi, J. P.; Diskin, G. S.; Fried, A.; Gilman, J. B.; Guo, H.; Hair, J. W.; Halliday, H. S.; Hanisco, T. F.; Hannun, R.; Hills, A.; Huey, L. G.; Jimenez, J. L.; Katich, J. M.; Lamplugh, A.; Lee, Y. R.; Liao, J.; Lindaas, J.; McKeen, S. A.; Mikoviny, T.; Nault, B. A.; Neuman, J. A.; Nowak, J. B.; Pagonis, D.; Peischl, J.; Perring, A. E.; Piel, F.; Rickly, P. S.; Robinson, M. A.; Rollins, A. W.; Ryerson, T. B.; Schueneman, M. K.; Schwantes, R. H.; Schwarz, J. P.; Sekimoto, K.; Selimovic, V.; Shingler, T.; Tanner, D. J.; Tomsche, L.; Vasquez, K. T.; Veres, P. R.; Washenfelder, R.; Weibring, P.; Wennberg, P. O.; Wisthaler, A.; Wolfe, G. M.; Womack, C. C.; Xu, L.; Ball, K.; Yokelson, R. J.; Warneke, C. Parameterizations of US Wildfire and Prescribed Fire Emission Ratios and Emission Factors Based on FIREX-AQ Aircraft Measurements. *Atmos. Chem. Phys.* **2024**, *24* (2), 929–956.
- (68) Collier, S.; Zhou, S.; Onasch, T. B.; Jaffe, D. A.; Kleinman, L.; Sedlacek, A. J.; Briggs, N. L.; Hee, J.; Fortner, E.; Shilling, J. E.; Worsnop, D.; Yokelson, R. J.; Parworth, C.; Ge, X.; Xu, J.; Butterfield, Z.; Chand, D.; Dubey, M. K.; Pekour, M. S.; Springston, S.; Zhang, Q. Regional Influence of Aerosol Emissions from Wildfires Driven by Combustion Efficiency: Insights from the BBOP Campaign. *Environ. Sci. Technol.* **2016**, *50* (16), 8613–8622.
- (69) Palm, B. B.; Peng, Q.; Fredrickson, C. D.; Lee, B. H.; Garofalo, L. A.; Pothier, M. A.; Kreidenweis, S. M.; Farmer, D. K.; Pokhrel, R. P.; Shen, Y.; Murphy, S. M.; Permar, W.; Hu, L.; Campos, T. L.; Hall, S. R.; Ullmann, K.; Zhang, X.; Flocke, F.; Fischer, E. V.; Thornton, J. A. Quantification of Organic Aerosol and Brown Carbon Evolution in Fresh Wildfire Plumes. *Proc. Natl. Acad. Sci. U. S. A.* **2020**, *117* (47), 29469–29477.
- (70) Garofalo, L. A.; Pothier, M. A.; Levin, E. J. T.; Campos, T.; Kreidenweis, S. M.; Farmer, D. K. Emission and Evolution of Submicron Organic Aerosol in Smoke from Wildfires in the Western United States. *ACS Earth Sp. Chem.* **2019**, *3* (7), 1237–1247.
- (71) May, A. A.; Lee, T.; McMeeking, G. R.; Akagi, S.; Sullivan, A. P.; Urbanski, S.; Yokelson, R. J.; Kreidenweis, S. M. Observations and Analysis of Organic Aerosol Evolution in Some Prescribed Fire Smoke Plumes. *Atmos. Chem. Phys.* **2015**, *15* (11), 6323–6335.
- (72) Pagonis, D.; Campuzano-Jost, P.; Guo, H.; Day, D. A.; Schueneman, M. K.; Brown, W. L.; Nault, B. A.; Stark, H.; Siemens, K.; Laskin, A.; Piel, F.; Tomsche, L.; Wisthaler, A.; Coggon, M. M.; Gkatzelis, G. I.; Halliday, H. S.; Krechmer, J. E.; Moore, R. H.; Thomson, D. S.; Warneke, C.; Wiggins, E. B.; Jimenez, J. L. Airborne Extractive Electrospray Mass Spectrometry Measurements of the Chemical Composition of Organic Aerosol. *Atmos. Meas. Technol.* **2021**, *14* (2), 1545–1559.
- (73) June, N. A.; Hodshire, A. L.; Wiggins, E. B.; Winstead, E. L.; Robinson, C. E.; Thornhill, K. L.; Sanchez, K. J.; Moore, R. H.; Pagonis, D.; Guo, H.; Campuzano-Jost, P.; Jimenez, J. L.; Coggon, M. M.; Dean-Day, J. M.; Bui, T. P.; Peischl, J.; Yokelson, R. J.; Alvarado, M. J.; Kreidenweis, S. M.; Jathar, S. H.; Pierce, J. R. Aerosol Size Distribution Changes in FIREX-AQ Biomass Burning Plumes: The Impact of Plume Concentration on Coagulation and OA Condensation/Evaporation. *Atmos. Chem. Phys.* **2022**, *22* (19), 12803–12825.
- (74) Clark, N.; Urbanski, S. P.; Goodrick, S. Smoke 101 and Differences Between Wildfire and Prescribed Fire Smoke in Western U.S.: Science You Can Use, 2024, p 8; <https://research.fs.usda.gov/treesearch/67647> (Accessed on August 15, 2024).

- (75) Kodros, J. K.; Kaltsonoudis, C.; Paglione, M.; Florou, K.; Jorga, S.; Vasilakopoulou, C.; Cirtog, M.; Cazaunau, M.; Picquet-Varrault, B.; Nenes, A.; Pandis, S. N. Secondary Aerosol Formation during the Dark Oxidation of Residential Biomass Burning Emissions. *Environ. Sci. Atmos.* **2022**, *2* (5), 1221–1236.
- (76) Nah, T.; Sanchez, J.; Boyd, C. M.; Ng, N. L. Photochemical Aging of α -Pinene and β -Pinene Secondary Organic Aerosol Formed from Nitrate Radical Oxidation. *Environ. Sci. Technol.* **2016**, *50* (1), 222–231.
- (77) Ding, J.; Dai, Q.; Zhang, Y.; Xu, J.; Huangfu, Y.; Feng, Y. Air Humidity Affects Secondary Aerosol Formation in Different Pathways. *Sci. Total Environ.* **2021**, *759*, No. 143540.
- (78) Jaffe, D. A.; O'Neill, S. M.; Larkin, N. K.; Holder, A. L.; Peterson, D. L.; Halofsky, J. E.; Rappold, A. G. Wildfire and Prescribed Burning Impacts on Air Quality in the United States. *Journal of the Air and Waste Management Association*. **2020**, *70* (6), 583–615.
- (79) Maji, K. J.; Li, Z.; Vaidyanathan, A.; Hu, Y.; Stowell, J. D.; Milano, C.; Wellenius, G.; Kinney, P. L.; Russell, A. G.; Odman, M. T. Estimated Impacts of Prescribed Fires on Air Quality and Premature Deaths in Georgia and Surrounding Areas in the US, 2015–2020. *Environ. Sci. Technol.* **2024**, *58* (28), 12343–12355.
- (80) U.S. Environmental Protection Agency (EPA). *National Emissions Inventory (NEI) Report*; Environmental Protection Agency, 2020. Available online: <https://www.epa.gov/air-emissions-inventories/national-emissions-inventory-nei> (accessed on August 15, 2024).
- (81) Goldstein, A. H.; Koven, C. D.; Heald, C. L.; Fung, I. Y. Biogenic Carbon and Anthropogenic Pollutants Combine to Form a Cooling Haze over the Southeastern United States. *Proc. Natl. Acad. Sci. U. S. A.* **2009**, *106* (22), 8835–8840.
- (82) McGlynn, D. F.; Barry, L. E. R.; Lerdau, M. T.; Pusede, S. E.; Isaacman-VanWertz, G. Measurement Report: Variability in the Composition of Biogenic Volatile Organic Compounds in a Southeastern US Forest and Their Role in Atmospheric Reactivity. *Atmos. Chem. Phys.* **2021**, *21* (20), 15755–15770.
- (83) Huang, R.; Hu, Y.; Russell, A. G.; Mulholland, J. A.; Odman, M. T. The Impacts of Prescribed Fire on PM_{2.5} Air Quality and Human Health: Application to Asthma-Related Emergency Room Visits in Georgia, USA. *Int. J. Environ. Res. Public Health* **2019**, *16* (13), 2312.
- (84) Li, C.; Misovich, M. V.; Pardo, M.; Fang, Z.; Laskin, A.; Chen, J.; Rudich, Y. Secondary Organic Aerosol Formation from Atmospheric Reactions of Anisole and Associated Health Effects. *Chemosphere* **2022**, *308*, No. 136421.
- (85) El Asmar, R. A Multi-Site Passive Approach for Studying the Emissions and Evolution of Smoke from Prescribed Fires [Data Set]. *Zenodo* **2024**, na.
- (86) El Asmar, R. Ground-Based Data from Field Studies in Southeastern US [Data Set]. *Zenodo* **2025**, na.